



University of Siena

Ph.D in Medical Genetics

Establishment and validation of a human cellular
model for CDKL5-related disorders

Mariangela Amenduni

Supervisor: Prof. Alessandra Renieri

Doctoral school in Oncology and Genetics

Academic year 2010-2011

Cicle XXIII

INDEX

ABSTRACT	2
1. INTRODUCTION	3
1.1 “ <i>CDKL5</i> -associated phenotypes”	8
1.2 Rett Syndrome	9
1.3 iPSCs to model human neurologic diseases	15
2. RATIONALE AND AIMS OF THE STUDY	19
3. RESULTS	23
3.1 “iPSC for <i>CDKL5</i> -related disorders”	24
Eur J Hum Genet .2011 Jul 13. doi:10.1038/ejhg.2011.131.	
3.2 Set up of a protocol for the analysis of morphological alterations in <i>CDKL5</i> neurons	38
3.2.1 Materials and methods	40
3.2.2 Results	42
3.3 Gene expression profiling of iPSCs from <i>CDKL5</i> patients	48
3.3.1 Experimental procedures	50
3.3.2 Results	52
4. DISCUSSION AND FUTURE PERSPECTIVES	55
5. REFERENCES	61
ACKNOWLEDGEMENTS	68

Abstract

CDKL5 is an highly conserved kinase expressed in a wide variety of cell-lines and tissues, with the highest levels in brain, testes and thymus. Mutations in this gene are responsible for the early-onset seizures variant of Rett syndrome and a severe encephalopathy with X-linked infantile spasms. However, the molecular mechanisms leading from *CDKL5* mutations to disease onset remain largely unknown and the protein is poorly characterized and its function partially elucidated so far. This is mainly due to the unavailability of both a mouse model and a good human cellular model. To overcome these limitations, we employed the approach of genetic reprogramming that allows the generation of *induced pluripotent stem* (iPS) cells directly from patients' fibroblasts. We successfully reprogrammed fibroblasts from 2 *CDKL5*-mutated patients (a male with p.T288I and a female with p.Q347X). In order to assess whether iPS cells are suitable as an *in vitro* model to study the pathogenesis of CDKL5-related disorders, we induced these cells toward a neuronal fate. Preliminary characterization of the neuronal differentiation process indicates that iPS cells can be differentiated into neurons and that the differentiation follows the stages observed in human embryonic stem cells (hESCs). No significant differences respect to neurons from normal controls have been observed. More detailed characterization of the obtained neurons is ongoing. Comparison of expression profiles between *CDKL5*-mutated and control iPSCs pointed out one interesting gene whose expression seems to be reduced in the absence of CDKL5.

1. INTRODUCTION

1. Introduction

Serine Threonine Kinase 9 gene (*STK9*), also known as *CDKL5*, was firstly isolated in 1998 by Montini E. and colleagues that were involved in a transcriptional mapping effort in the Xp22 region ¹. In 2003 Kalscheuer and colleagues have revisited the complete gene structure of *STK9* reporting some discrepancies with the exon number and sizes indicated by Montini in 1998 ^{1,2}. The main difference is that *STK9* contains at least 23 exons, with the first three exons (1, 1a and 1b) being untranslated and determining two splice variants with different 5'UTRs (Fig. 1A). Splice variant I, containing exon 1 is the more abundant while splice variant II, containing exon 1a and 1b is transcribed at very low levels ².

CDKL5 (OMIM #300203), located on Xp22, encodes for a serine-threonine kinase with an N-terminal domain highly homologous to members of the mitogen-activated protein (MAP) and cyclin dependent kinase (CDK) families ³. *CDKL5* is a large protein of 1030 aminoacids with an estimated molecular weight of 115 kDa containing a conserved serine-threonine kinase domain within its N-terminus and a large C-terminal region (Fig 1B). It is highly conserved and ubiquitously expressed in a wide variety of cell lines and tissues, with the highest level in brain, testes and thymus ³.

Very recently an additional exon (16b) within the *CDKL5* gene has been identified, showing no homology with other sequences in the human genome and an extremely high level of similarity between species, indicating a functional role that has been conserved during evolution ⁴. It encodes a further 41 aa, producing a predicted protein of 120 kDa in humans. This new transcript has been detected also in mouse brain, with different levels in the various regions, whereas it is not found in other organs, thus suggesting the potential functional importance of the isoform in brain. However the full-length protein containing exon 16b has not yet been identified in tissues, neither by western blotting analysis nor by immunofluorescence studies in human fibroblasts or mouse tissues. Authors suggest that these results do not indicate that the protein is not expressed, but may be due to its low amount that cannot be detected by the methods used. Despite these findings, the presence of the 16b-containing mRNA isoform in all brain regions of adult mouse is in favour of the expression of the long *CDKL5* isoform *in vivo* ⁴. Furthermore another recent publication has reported a novel *CDKL5* splice variant containing intron 18 (designated as *CDKL5*₁₀₇) and encoding a protein with an alternative C-terminus in both human and mouse. This novel transcript (exon1-intron 18) is widely expressed in all human tissues and cell lines examined,

and is the predominant isoform in human brain. In view of these results it has been ascertained whether its functional characteristics, such as the catalytic activity and subcellular localization, are similar to those of the CDKL5₁₁₅ isoform. The detailed characterization revealed that its subcellular distribution is largely maintained with respect to CDKL5₁₁₅ isoform, that its autophosphorylation and heterophosphorylation activity is reduced, but this is compensated by an increase in protein level. Interestingly, this isoform seems to be more stable and resistant to proteasome degradation than the CDKL5₁₁₅ isoform⁵. However, it has to be taken into consideration that the significance of these *in vitro* studies for brain function could be better clarified only by studies *in vivo* and on the primarily affected tissue.

Since its molecular characterization started in 2005, when mutations in this gene were identified in patients affected by Rett Syndrome (RTT), CDKL5 protein remains still rather uncharacterized. Its involvement in RTT has been explained by the fact that this kinase seems to work in a molecular pathway common to that of MeCP2, the main gene responsible for RTT⁶⁻⁸. It has been demonstrated that the two proteins interact both *in vivo* and *in vitro* but there are some controversial results regarding the functional role of this interaction; in fact an *in vivo* phosphorylation of Mecp2 has been reported by Mari and colleagues, but the result has not been confirmed by Li and colleagues^{3,6,7}

Intriguingly the two genes show an overlapping temporal and spatial expression profile in brain and are simultaneously activated during neuronal maturation⁶. Moreover, the two proteins bind to different regions of the N-terminal domain of Dnmt1 strengthening the hypothesis of their belonging to the same molecular pathway⁹. More recently Carouge and colleagues addressed the question of the transcriptional control of Cdkl5 by Mecp2 as a potential link between the two genes, taking advantage of MeCP2 induction by cocaine in rat brain structures⁸. Their data reveal that over-expression of Mecp2 in transfected cells results in the repression of Cdkl5 expression and that *in vivo* Mecp2 directly interacts with *Cdkl5* gene in a methylation-dependent manner. Taken together these results are consistent with Cdkl5 being a Mecp2-repressed target gene and provide new insights into the mechanism by which mutations in the two genes result in overlapping neurological symptoms⁸.

At the moment, CDKL5 function during neuronal maturation and activity remains still rather uncharacterized. However since mutations in *CDKL5* and *MECP2* lead to similar genetic disorders the relationship between these two genes has been extensively investigated. MeCP2 is induced during embryogenesis and its levels remain rather homogeneous during postnatal development until adulthood¹⁰⁻¹². On the contrary, CDKL5 is highly expressed later in development, and its levels are much more modulated than those of MeCP2, despite an

overlapping expression profile of these two proteins ¹³. Moreover, while MeCP2 is an exclusively nuclear protein, CDKL5 shuttles between the nuclear and cytoplasmic compartments. Interestingly cytoplasmic CDKL5 is localized in the dendritic branches with a distinct punctuate staining. It is noteworthy that CDKL5 expression is mainly cytoplasmic in late embryonic stages of mouse brains, with a low fraction of the protein in the nucleus. The nuclear fraction increases during early postnatal stages consistently with neuronal maturation and remains as such until adult stages ¹³. These data suggest that CDKL5 functions might be modulated through mechanisms regulating its shuttling between nucleus and cytoplasm. Intriguingly, it has been demonstrated a fundamental role of the C-terminal tail in regulating CDKL5 function by affecting its stability, kinase activity and its dynamic subcellular distribution ^{3,7,13}. Further studies have showed that CDKL5 co-localizes and is associated with a number of splicing factors that are stored in structures called nuclear speckles, in both cell lines and tissues. In these structures CDKL5 seems to manage the nuclear trafficking of splicing factors and thus indirectly of the splicing machinery ¹⁴. It is already known that phosphorylation of the RS domain of Serine-rich (SR) splicing factors is necessary to release these factors from speckles and direct them to sites where pre-mRNA processing takes place. Considering that several protein kinases have been described to be able to phosphorylate the RS domain of SR proteins Ricciardi and colleagues have hypothesized that also CDKL5 could have a role in nuclear speckles organization. Interestingly it has been demonstrated that CDKL5 acts on nuclear speckle disassembly determining a redistribution of at least some speckle proteins. ¹⁴.

In spite of all these findings, our knowledge of the function of CDKL5 inside the neuron and of the underlying molecular mechanisms is still limited by the unavailability of both a mouse model and a good human cellular model for CDKL5-related disease. A recent study in cultured rat cortical neurons has partially overcome this limitation and has demonstrated that CDKL5 down-regulation by RNA interference inhibits neurite outgrowth and dendritic arborization, while its over-expression elicits the opposite effect ¹⁵. In several studies CDKL5 has been found to exert its function in the nucleus, while other groups have reported a consistent expression of CDKL5 in the dendrites of cultured neurons, thus suggesting that it might have a cytoplasmic function independent of its role in the nucleus ^{3,7,13}. Starting from these data Chen and colleagues have inspected its subcellular localization in rat neurons. Interestingly CDKL5 was detected at high levels in the cytoplasmic fraction of cultured cortical neurons. Moreover, immunostaining experiments revealed that it co-localizes with F-actin in the peripheral domain of growth cones, indicating a possible role in actin

cytoskeleton regulation. Since Rho GTPases are involved in actin dynamics and neuronal morphogenesis, authors hypothesized a possible interaction with CDKL5. In fact, colocalization and GST pull-down assays revealed that CDKL5 directly or indirectly interacts with Rac1 and that this interaction is enhanced by brain-derived neurotrophic factor (BDNF). The finding that CDKL5 regulates neuronal morphogenesis through a mechanism involving Rac1-BDNF signaling might represent a novel mechanism involved in the pathology of CDKL5 related disorders¹⁵.

The recent research recapitulated above has given important glimpses on CDKL5 role in brain. However, due to the absence of a good human cellular model, it has not been possible to date to verify whether all these findings resemble the situation in affected human brain. All the information achieved so far about CDKL5 indicates that it exerts different functions based on the intracellular compartment in which it is localized. However, CDKL5 function is far from being unravelled, precluding an understanding of its role in the pathogenic processes responsible for disease onset.

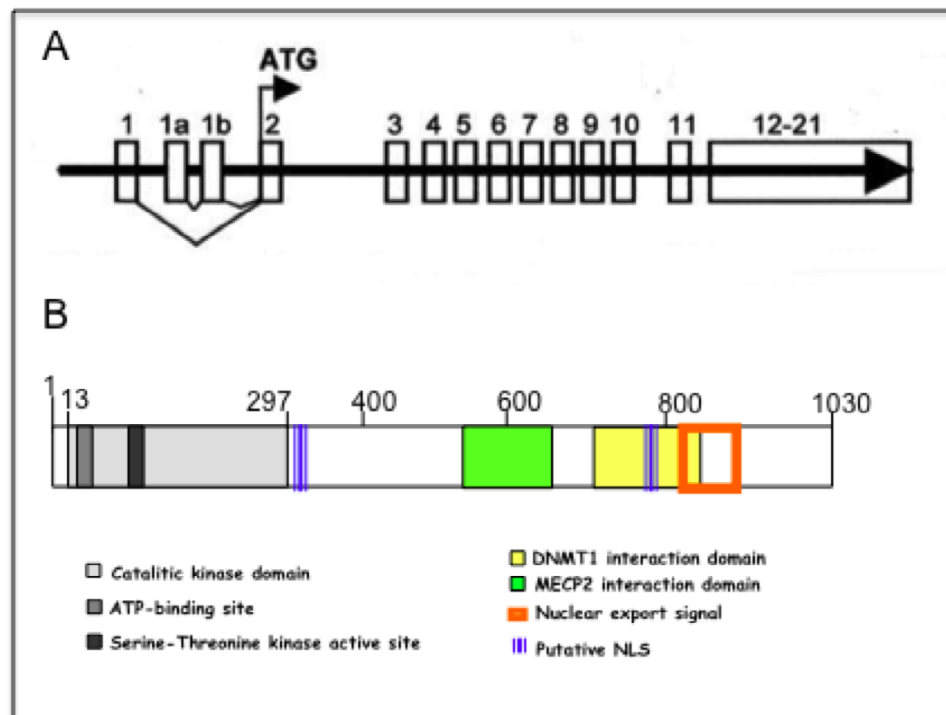


Fig. 1. CDKL5 gene and protein. (A) Genomic structure of *CDKL5* gene (previously known as *STK9*) with exons 1, 1a and 1b. The translation start codon ATG is contained in exon 2. Image modified from Kalscheuer et al., 2003². (B) Schematic representation of the CDKL5 protein with its functional domains.

1.1 “*CDKL5*-associated phenotypes”

Several groups have described mutations in *CDKL5* in patients with seizures appearing soon after birth and severe mental retardation. The triad of infantile spasm, hypsarrhythmia and severe mental retardation is characteristic of West syndrome or, when X-linked, infantile spasm syndrome (ISSX). The first alterations in this gene have been reported in two unrelated girls with ISSX and X-autosome translocations. In both cases the breakpoints disrupted the *CDKL5* gene². After that, mutations in *CDKL5* have been identified in patients diagnosed with atypical Rett syndrome (RTT), a girl with an autistic disorder and intellectual disability and a boy with severe, early infantile onset neurological disorder¹⁶⁻¹⁸. Additionally a boy with severe epileptic encephalopathy and bilateral cataract was shown to have an interstitial deletion comprising the *CDKL5* gene¹⁹. In summary, the phenotypic spectrum of *CDKL5* abnormalities has progressively expanded to include clinical features resembling those of other neurodevelopmental disorders. In particular, most of the cases have been diagnosed with the early-onset seizures variant of RTT suggesting that this could be the predominant phenotype caused by *CDKL5* mutations^{17,20}.

The hallmarks of *CDKL5*-associated diseases are early-onset intractable seizures with infantile spasms, severe intellectual disability and atypical RTT features. The common feature describing patients affected by the “early-onset seizures variant” of RTT is the appearance of epilepsy during the very first weeks of life and a developmental delay without any period of normal development; in many cases epilepsy becomes refractory to treatment during later stages²¹. Moreover, *CDKL5* mutated patients clearly exhibit some RTT-like features such as deceleration of head growth, stereotypies and hand apraxia, and sleep disturbances²²⁻²⁴. Most patients show a combination of different hand stereotypies without hand gaze and bruxism, although these features become really evident in patients at older age and also able to walk with support. Conversely, dysautonomic features such as breathing disturbances and gastrointestinal dysfunction are rare suggesting a possible better preserved autonomic system in patients with *CDKL5* mutations compared with typical RTT ones²⁵.

Although the epileptic disorder is the key feature to identify patients likely to present *CDKL5* mutations, there is limited information regarding its precise electro-clinical phenotype. Buoni and colleagues in 2006 described an epileptic pattern consisting of myoclonic epilepsy with refractory seizures and a “unique electroencephalogram (EEG) pattern”²⁶. Archer and colleagues have further extended the description of the epilepsy

phenotype suggesting that the spectrum of severity of the seizure disorder is broader, ranging from no seizures at all to hundreds of seizures a day. However, it is interesting to note that also in the patients described by Archer, seizures are largely resistant to drug treatment ²⁰. Recently another contribution to the definition of the epileptic phenotype in *CDKL5* mutations came from Bahi-Buisson and colleagues ²¹. They investigated the electro-clinical pattern of ISSX patients in order to give a better characterization of the phenotype and thus to facilitate an early diagnosis. Their data suggest an epilepsy phenotype with a three-stage pattern that initiates with “early epilepsy”, moves on to epileptic encephalopathy and comes to an end with late multifocal and myoclonic epilepsy ²¹.

1.2 Rett syndrome

Since the early-onset seizures variant of RTT is considered the predominant phenotype caused by *CDKL5* mutations, this syndrome will be described in further details ^{17,20}.

Rett syndrome (OMIM#312750) is a progressive neurodevelopmental disorder almost exclusively affecting females with an incidence of 1:10000 born females. Due to its incidence it represents the second cause of mental retardation in girls ^{27,28}. The syndrome was first described by Andreas Rett in 1966, but it was internationally recognized as a distinct clinical entity when Hagberg et al. described 35 new cases in 1983 ²⁹. In the classic form, Rett girls are characterized by a period of 6-18 months of apparently normal development after which they present a developmental arrest followed by regression in language and motor skills. They usually have normal head circumference at birth followed by postnatal deceleration of head growth leading to microcephaly by the second year of life. As the syndrome progresses, patients lose the purposeful use of hands and develop repetitive stereotypic hand movements. The pattern consists of tortuous hand wringing, hand washing, clapping, flapping or other more bizarre hand automatisms ³⁰. Patients also manifest social withdrawal, communication dysfunction, loss of acquired speech and cognitive impairment, in addition to irritability and self-abusive behaviour. Further characteristics are the appearance of autistic features, including a reduction in interpersonal contact, hypersensitivity to sound, indifference to the surrounding environment and unresponsiveness to social cues ^{28,31}. RTT girls also suffer devastating motor deterioration with the development of ataxia and gait apraxia. Most girls with RTT develop seizures ranging from easily controlled to intractable epilepsy, and suffer respiratory dysfunctions, bruxism and impairment of sleeping patterns. Amelioration of the

autistic-like behaviour occurs between 5 and 10 years of age, but other somatic and neurological handicaps, such as severe scoliosis, rigidity and reduced somatic growth become evident during this period. As patients get older they develop Parkinsonian features. The condition reaches a plateau and, although sudden death can occur, most people with Rett syndrome survive up to the sixth or seventh decade of life in a profoundly debilitated physical condition ^{28,31}.

As experience on this syndrome increased it has become evident that females with RTT may present with a much broader phenotype than originally described. Indeed atypical forms of RTT have been described, with significant differences in disease onset, severity of impairment and profile of clinical course ^{22,27}. The milder forms of RTT include **the late regression variant**, which is rare and still controversial, and **the “forme fruste” variant** presenting with a later age of onset and regression occurring between 1 and 3 years of age. Another form of RTT with a benign course is **the Zappella variant** previously known as the **Preserved Speech Variant (PSV)**. Affected girls recover the ability to speak in sentences, although not necessarily in context, and display an improvement of purposeful hand movements. The more severe variants include **the congenital form**, in which girls appear floppy and retarded since the very first months of life, thus lacking the early period of normal development typical of classic RTT, and **the early-onset seizures variant** with severe epileptic seizures appearing soon after birth.

Considering that RTT occurred almost exclusively in females, an X-linked dominant inheritance was suggested, with possible male lethality. However, since more than 99% of RTT cases are sporadic, it was very difficult to map the disease locus by traditional linkage analysis. Using information from rare familial cases, exclusion mapping identified the Xq28 candidate region, and subsequent screening of candidate genes in RTT patients detected mutations in *MECP2* gene (Methyl-CpG-binding Protein 2, OMIM #300005). The spectrum of *MECP2* mutations includes missense, nonsense and frameshift mutations with over 300 unique pathogenic nucleotide changes described (<http://mecp2.chw.edu.au/>; <http://biobank.unisi.it>) ^{32,33}, together with deletions encompassing whole exons ³⁴. Eight recurrent missense and nonsense mutations account for 70% of all changes, while small C-terminal deletions account for another 10%, and complex rearrangements represent 6%. Although RTT was initially believed to occur only in females, this dogma was broken with the identification in males of *MECP2* mutations causing a variable phenotype ³⁵. The phenotypes observed in males can be divided in three categories: i) presence of severe

neonatal encephalopathy. Soon after birth there is severe neurodevelopmental delay and the boys die during early childhood. These male patients bear *MECP2* mutations that are also detected in RTT girls; ii) presence of symptoms that are highly similar to those observed in classic RTT females^{36,37}. This phenotype results from somatic mosaicism for severe mutations or occurs in males presenting a 47XXY karyotype^{38,39}; iii) presence of a phenotype ranging from moderate non specific to severe and syndromic mental retardation or psychiatric disorders⁴⁰⁻⁴². These patients usually carry *MECP2* mutations that have never been found in RTT girls. Furthermore duplications in Xq28 region including *MECP2* have been identified in males as the cause of mental retardation and progressive neurological symptoms^{43,44}.

MECP2 mutations are detected in about 95% of classic RTT patients and in 20-40% of variant cases. Since in some RTT patients no *MECP2* mutations could be found, it was proposed that there was at least another gene on the X chromosome responsible for atypical RTT. Indeed in 2005, mutations in *CDKL5* were detected in patients with a phenotype overlapping the early-onset seizures variant of RTT⁶. So far, *CDKL5* disease-causing mutations include chromosome translocations, deletions, insertions, non-sense mutations causing premature termination of transcription, or missense mutations generally occurring within the catalytic domain resulting in decreased catalytic activity¹³. Over 50 different pathogenic *CDKL5* mutations have been described, 27 of which resulting in the premature truncation of the protein due to nonsense or frame-shift mutations (RettBASE-<http://mecp2.chw.edu.au>)³².

Despite intense research efforts no mutations in *MECP2* and *CDKL5* have been identified for many RTT variant patients, suggesting the involvement of one or more additional genes. In 2008, by array-CGH analysis our group identified a de novo interstitial deletion of chromosome 14 including only five genes in a patient with a complex phenotype classified as RTT-like (<http://www.biobank.unisi.it>). By mutation screening for these genes in RTT patients negative for both *MECP2* and *CDKL5* mutations our group identified mutations in *FOXG1B* in patients with a phenotype compatible with the congenital variant of RTT⁴⁵. Soon after that, several other groups have identified mutations in *FOXG1* in patients fulfilling the criteria of the congenital variant⁴⁶⁻⁴⁸. So far 17 molecular alterations in *FOXG1*, including 10 point mutations, have been reported. Patients with *FOXG1* mutations usually present with impaired motor development and absence of voluntary hand use. In contrast with the classic form of RTT, patients exhibit poor eye contact, continuous stereotypic hand movements with hand-washing and hand-mouthing activities and several of them have abnormal tongue

movements as well as jerky movements of the limbs ⁴⁹. Scoliosis and autonomic neurovegetative symptoms typical of RTT are frequently present ⁴⁶.

MECP2

MeCP2 protein is encoded by a four-exon gene mapping in Xq28. Alternative splicing of exon 2 generates two different isoforms of the protein that differ only in their N-termini. The first isoform (MeCP2A) uses a translational start site within exon 2, whereas the other isoform (MeCP2B) derives from an mRNA in which exon 2 is skipped and a new in-frame ATG in exon 1 is used ^{50,51}. Expression studies in mice demonstrated that MeCP2B is predominantly expressed in brain, while MeCP2A is more abundant in other tissues ⁵¹. MeCP2 is a member of the methyl-CpG binding protein family and is composed of three functional domains: the methyl-CpG binding domain (MBD), the transcriptional repression domain (TRD) and a C-terminal domain, together with two nuclear localization signals (NLS) (Fig 2.). The MBD binds to symmetrically methylated CpG islands, while the downstream TRD is able to recruit co-repressor complexes that mediate gene silencing through deacetylation of core histones ⁵². MeCP2 exerts its function as a transcriptional repressor either through interaction with the corepressor Sin3A and the histone deacetylase complex or through interaction with c-Ski and N-CoR, remodelling chromatin that becomes inaccessible to the transcriptional machinery ^{53,54}. In addition, MeCP2 is able to perform histone deacetylase-independent transcriptional repression through the interaction of the TRD domain with the transcription factor TFIIB ⁵⁵. Furthermore it has been demonstrated that MeCP2 interacts *in vivo* with Y box-binding protein 1 in an RNA-dependent manner and acts as a splicing regulator ⁵⁶. Integrated genome-wide promoter analysis of MeCP2 binding, CpG methylation, and gene expression studies unexpectedly revealed that the majority of MeCP2-bound promoters are on active genes and that the promoters with the highest methylation levels are not bound by MeCP2 ⁵⁷. These results contrasted the idea that the primary function of MeCP2 is the silencing of methylated promoters and suggested that MeCP2 is a “transcriptional regulator” rather than a “transcriptional repressor”.

To uncover the molecular mechanisms leading from *MECP2* mutations to RTT onset, different mouse models have been generated, all presenting with clinical manifestations similar to RTT, and extensively characterized ^{10,58-60}. These models have contributed to the identification of specific alterations in glutamatergic neurons. Indeed, Chao et al. in 2007

demonstrated that glutamatergic neurons lacking *Mecp2* display a 46% reduction in synaptic response whereas neurons with doubling of *Mecp2* exhibit a two-fold enhancement in synaptic response. Further analysis showed that these changes were primarily due to the number of synapses formed. All together these data indicate that MeCP2 function is critical at the single neuron level and that this protein is crucial in regulating glutamatergic synapse formation in early postnatal development. Despite these results it has not been experimentally demonstrated that RTT is exclusively due to the lack of functional MeCP2 in neurons. To this respect Ballas et al have demonstrated that loss of MeCP2 occurs also in glial cells resulting in a toxic effect on the neighbouring neurons. In fact, using an in vitro co-culture system they have observed that mutant astrocytes from a RTT mouse model are not able to support normal dendritic morphology of either wt or mutant hippocampal neurons. These data suggest that astrocytes with MeCP2 mutations have a non-cell autonomous effect that causes the neuronal damage, probably due to aberrant secreted factors ⁶¹.

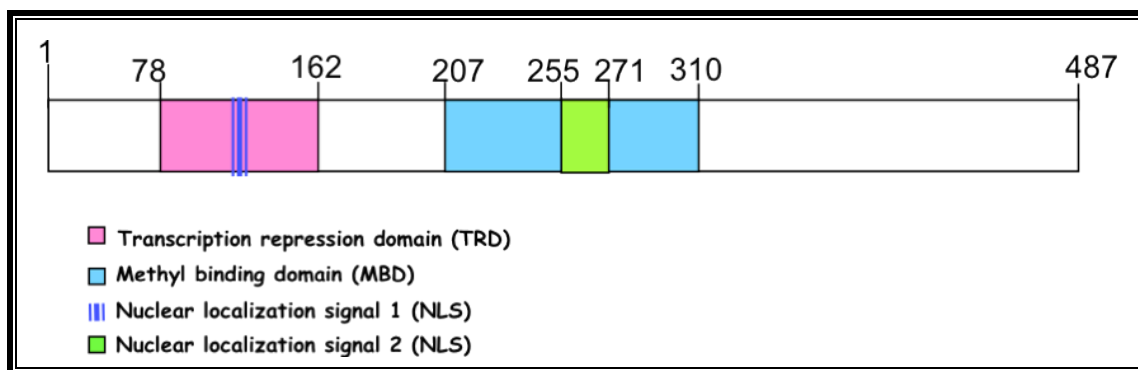


Fig. 2. MeCP2 protein structure with its functional domains. The numbers refers to amino acid positions.

FOXG1B

FOXG1B encodes for a transcriptional repressor expressed only in fetal and adult brain and testis, namely forkhead box protein G1, FoxG1. This protein interacts with the transcriptional repressor JARID1B and with transcriptional corepressors of the Groucho family and through this interaction it plays a fundamental role in early brain and telencephalon development (Fig.3). Moreover, like MeCP2, FoxG1 associates indirectly with the histone deacetylase 1 protein ⁶². Despite its early expression in telencephalon, Foxg1 has

also been detected in the differentiating cortical compartment in postnatal stages, although at lower levels, suggesting that it may have additional functions in differentiating and mature neurons ⁴⁵. Interestingly FoxG1 expression profile coincides with that of MeCP2 in differentiating and mature neurons and the two proteins share some analogies in their molecular function, suggesting that they can participate into the same molecular pathway. As concerns their subcellular localization FoxG1 localizes in the nuclear compartment, but is excluded from the heterochromatic foci, positive for MeCP2; this finding suggests that, differently from MeCP2, FoxG1 is not a transcriptional repressor stably bound to heterochromatin ⁴⁵. However the two proteins co-localize in the nuclear compartments outside the heterochromatic foci, thus suggesting that they may belong to a common complex as already demonstrated for MeCP2 and CDKL5. Intriguingly, it has recently been demonstrated that the FOXG1 mutant protein p.R244C localizes in the nuclear speckles suggesting that this specific localization might influence the function of these nuclear domains, involved in the pre-mRNA processing in cells. Considering that also the product of *CDKL5* gene localizes in nuclear speckles ¹⁴, further studies will be required to clarify the functional consequences of the localization of mutant FOXG1 protein in nuclear speckles and to shed light on the possible link with CDKL5.

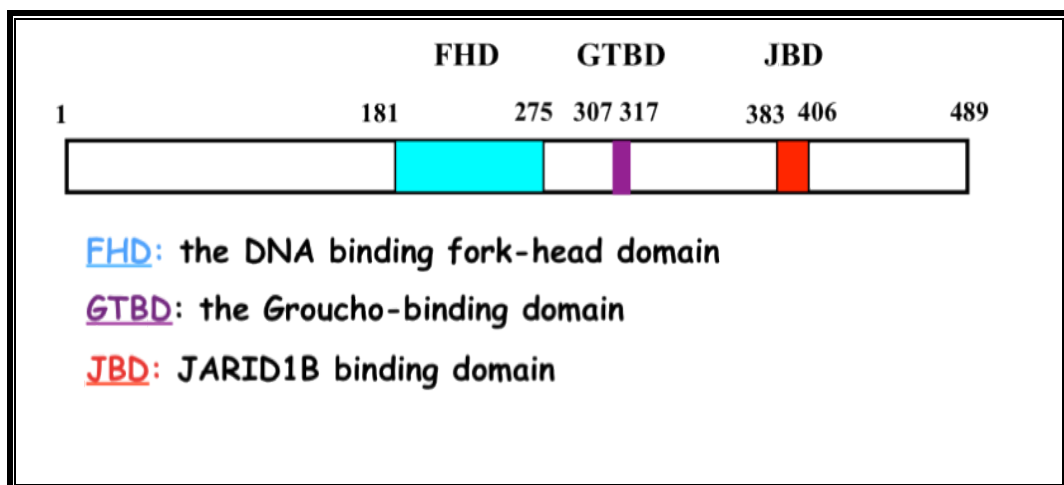


Fig. 3. Schematic representation of the FoXG1 protein with its functional domains. The numbers at the top refers to amino acids positions.

1.3 iPSCs to model human neurologic diseases

Even with intensive research efforts, the clarification of the molecular mechanisms of RTT, as well as other neurodevelopmental and neurodegenerative diseases, has been hampered by the lack of satisfactory human *in vitro* cellular models. Most of our understanding of neurologic disorders has been obtained from the study of mutant mouse models. However this approach is limited to monogenic disorders and mouse models do not always faithfully recapitulate human conditions. Moreover, they do not evaluate the influence of genetic background on disease phenotype. Important breakthroughs on disease-related neuronal phenotypes in humans have been achieved from analysis of post mortem tissues; however, these tissues often represent the end-stage of disease and therefore are not a faithful representation of the disease pathogenesis⁶³. A completely new perspective for the creation of patient- and disease-specific human cellular models has been opened by the development in 2007 of induced Pluripotent Stem Cells (iPSCs)⁶⁴. iPSCs can be derived from differentiated somatic cells, mainly from skin fibroblasts, through forced expression of a set of transcription factors related to pluripotency, most commonly consisting of *OCT-4*, *SOX-2*, *c-MYC* and *KLF-4*⁶⁴⁻⁶⁷. iPSCs are considered functionally and molecularly very similar to human Embryonic Stem Cells (hESCs) in terms of morphology, proliferation, surface markers, gene expression, promoter activities, telomerase activities, *in vitro* differentiation potential and teratoma formation. Like hESCs, they can be expanded indefinitely and differentiated *in vitro* into many different cell types⁶⁴. These features make them the ideal tool to study disease mechanisms directly on the primarily affected cells, especially for disorders of the nervous system, where issues of accessibility and the inability of mature neurons to regenerate limit the direct study of human diseased tissue. Furthermore iPSCs, thanks to their unlimited growth potential, can offer the opportunity to perform large-scale drug screening for the identification of new therapeutics and they might represent an ideal source of autologous cells for replacement therapies (Fig 4). To pursue all these aims however the fundamental question that has to be addressed is whether or not iPSCs, like hESCs can be efficiently differentiate into functional cell of various lineages.

Great interest has recently arisen on the possibility to model neurodevelopmental and neurodegenerative disorders using iPSCs, thus bypassing the main issue of inaccessibility of the nervous system. To this purpose several groups have performed comparison studies between iPSC and hESC, in order to test whether the process of differentiation of iPSCs into

committed neural stem cells and subsequently into functional neurons was similar to hESCs^{68,69}. It was already established that hESC-derived neuroepithelial cells (NE) differentiate into neurons in the first month of the differentiation course, and into astrocytes and oligodendrocytes after 2-3 months. Hu and colleagues demonstrated that iPSCs follow the same order and timing of neurogenesis and gliogenesis of hESCc and normal brain development regardless of if the iPSCs were from adult or neonatal cells, if they were generated by transfection with 3 or 4 genes, or if the iPSCs were derived with or without transgene integration^{68,70,71}. Moreover, it has been observed that human iPSCs can be patterned in response to morphogens to neurons with specific regional identities of the CNS using methods established for hESC-derived neurons⁷¹⁻⁷³. Finally, it has been demonstrated that iPSCs are able to differentiate into functional neuronal subtypes such as glutamatergic, GABAergic and dopaminergic neurons. Indeed, iPSCs-derived motor-neurons are electrophysiologically active and may form functional synapses with surrounding neurons, with a maturation process similar to that observed in hESC-differentiated neurons^{68,71}. Similarly, iPSCs can be differentiated into functional A9 dopaminergic neurons similar to hESC-derived neurons in terms of time course, neural patterning and efficiency of dopaminergic neurons generation^{69,74}.

Another interesting issue regarding iPSCs compared to hESCs is represented by the epigenetic status of the somatically silenced X chromosome in female cells. As concerns female hESC lines it seems that there is a highly variable epigenetic status of the X chromosome, even among the same line at different passages, under varying culture conditions or among subclones⁷⁵. Regarding iPSCs, different groups have recently demonstrated that iPSCs retain an inactive X-chromosome in a non-random pattern in contrast with mouse iPSCs that reactivate the inactive X-chromosome after reprogramming and exhibit random XCI upon differentiation^{66,75,76}. Interestingly Marchetto and colleagues showed X-inactivation is erased in reprogrammed iPSC clones and subsequently restored during neuronal differentiation⁶³. The reasons for this discrepancy remain to be elucidated but a possible effect of differences in reprogramming methods and culturing of iPSCs has been hypothesized⁷⁶. However, despite these results, the maintenance of XCI in the majority of female iPSCs makes these cells an ideal source for the isolation of isogenic control and experimental iPSC lines to study X-linked disorders such as RTT, thus overcoming the main disadvantage of other cellular models in which cultures are mosaic of cells expressing the WT allele and cells bearing the mutated one.

Up to now, reprogramming of fibroblasts for several neurodegenerative (ALS, SMA, Parkinson, HD, FD) and neurodevelopmental (FRAXA, PW-AS) disorders has been reported, but few studies have actually recapitulated the phenotype of disease in the iPSC-derived neuronal population. Interestingly, iPSC-derived motor neurons from a single SMA patient showed a decrease of survival after 6 weeks of differentiation compared with normal control⁷⁷, while iPSCs derived from three FD patients revealed a defect in neuronal differentiation and migration⁷⁸. These neuronal phenotypes are consistent with alterations identified in patients confirming the potential of this technology to model neurological disorders. ALS and Parkinson's disease have also been studied using iPSCs and neuronal differentiation, but no phenotype as yet been observed or reported, suggesting that more subtle analyses will be necessary to reveal phenotypes of diseases with late onset^{79,80}. As concerns Rett syndrome, iPSCs have been recently generated from *MECP2* mutated patients fibroblasts and differentiated into glutamatergic neurons^{63,76}. In particular, Marchetto and colleagues reported that RTT glutamatergic neurons exhibit a reduced number of synapses and dendritic spines when compared with those derived from control iPSCs or hESCs. Additionally, electrophysiological recordings from RTT neurons revealed an important reduction in the frequency and amplitude of spontaneous excitatory and inhibitory postsynaptic currents. It is worthwhile to note that these findings are in accordance with the data on mouse models, thus confirming the applicability of iPSCs technology to model in vitro a neurological and cognitive disorder such as RTT. Cheung A and colleagues, that derived iPSCs from a patient with a functionally null mutation in *MECP2*, obtained similar results⁷⁶. Indeed they demonstrated that iPSCs retain an inactive X chromosome in a non-random pattern, and this status is maintained upon differentiation into neurons, thus highlighting the possibility to obtain isogenic controls from the same patient eliminating the variance of genetic background between individuals. Furthermore a morphological analysis of iPSCs-derived neurons revealed a significant soma size reduction in the mutant compared to the isogenic control in agreement with previous findings⁶³.

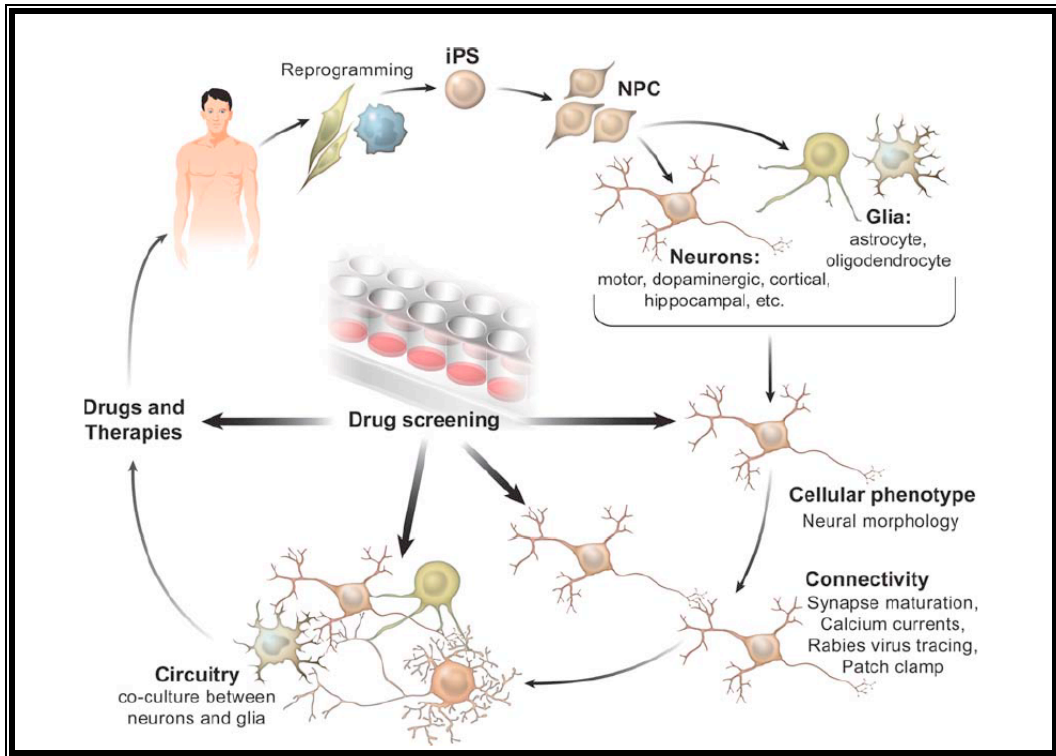


Fig. 4. iPSC technology and its role in neurodegenerative and neurodevelopmental diseases modeling. Human iPSCs are generated after reprogramming of somatic cells derived from patients and normal controls. iPSCs can be subsequently differentiated into specific neuronal subtypes. Detailed phenotypic analysis is performed to evaluate disease-associated defects (neuronal morphology, connectivity and circuitry integration). Once a recognizable phenotype is identified, these cells can be used to develop large scale drug screenings for the identification of new therapeutic compounds, potentially benefiting the patient. (Image taken from Marchetto et al., 2010⁷⁹).

2. RATIONALE AND AIMS OF THE STUDY

2. Rationale and Aims of the study

CDKL5 is the gene responsible for the early-onset seizures variant of Rett syndrome and a severe encephalopathy with X-linked infantile spasms. However, the molecular mechanisms leading from *CDKL5* mutations to disease onset remain largely unknown and the protein is poorly characterized and its function partially elucidated so far. This is mainly due to the absence of satisfactory in vitro human cellular models. In order to clarify the role of *CDKL5* in human affected neurons and establish an innovative cellular model of the disease we decided to employ the approach of genetic reprogramming that allows generating induced pluripotent stem cells (iPSCs) directly from patients fibroblasts. To reach this ambitious aim, we have reprogrammed fibroblasts from 2 patients with *CDKL5* mutations (a male with a p.T288I and a female with and p.Q347X mutation, respectively) into iPSCs. In order to assess whether these cells are suitable as an in vitro model to study the pathogenesis of *CDKL5*-related disorders, we induced the iPSCs toward a neuronal fate, following a protocol established for human ESCs (Result 1).

iPSC technique has already been applied in the attempt to model several neurodegenerative and neurodevelopmental disorders; however only few studies have actually recapitulated the phenotype of disease in the iPSC-derived neuronal population. In most cases the demonstration of disease-specific pathogenesis and phenotypic rescue in relevant cell types is a current challenge in the field ⁷⁹. An interesting example of a neurodevelopmental disease with promising results concerning disease modelling by iPSC technology is Rett syndrome. As a matter of fact iPSCs have recently been generated from fibroblasts of patients carrying different *MECP2* mutations and further differentiated into glutamatergic neurons. Neurons derived from RTT patients exhibit functional and morphological alterations of the synapses and thus have also been used to test the effects of drugs in rescuing synaptic defects ⁶³. Interestingly iPSCs-derived neurons carrying different *MeCP2* mutations exhibit a decrease in cell soma size when compared to normal controls, in agreement with the recent results obtained by Cheung and colleagues ⁷⁶. Indeed, in patients with neurodevelopmental disorders such as nonsyndromic mental retardation and RTT an abnormal morphology is a characteristic feature of neurons ⁸¹.

It is already well established that mutations in *MECP2* and *CDKL5* are both associated with a RTT phenotype and that the two proteins seem to work in a common molecular pathway. Starting from this consideration it is interesting to ascertain whether *CDKL5*-mutated neurons present the same or different morphological defects with respect to *MECP2*-mutated neurons. Indeed, it has recently been demonstrated that in rat brain *cdkl5* is essential for neuronal morphogenesis since its absence inhibits neurite growth and dendritic arborization¹⁵. Starting from these data we decided to investigate whether *CDKL5*-iPSCs derived neurons exhibited any significant morphological alteration, in order to validate the data obtained by Chen and colleagues in a human cellular model for *CDKL5* and eventually confirm the phenotype observed in *MECP2* iPSCs-derived neurons. Considering that neural differentiation results in variable and heterogeneous cultures of neurons, glia and undifferentiated cells, we decided to test two different lentiviruses in order to establish which one was more efficient in the visualisation of neuronal morphology: an ubiquitous one named PLL 3.7 and a neuro-specific lentivirus under the control of synapsin promoter, namely Syn-EGFP. Furthermore we performed cell soma size analysis comparing mutated neurons with normal controls (Results 2).

Several studies have underlined so far the possibility that *CDKL5* performs *MeCP2*-independent functions. The fact that the autonomous nervous system, whose malfunction in patients with *MECP2* mutations causes severe respiratory problems and constipation, appears to be better preserved in patients with *CDKL5* alterations supports separate functions for the two proteins⁸². At the same time mutations in *CDKL5* are associated with some severe neurological symptoms that are occasionally reported in typical *MeCP2* cases, such as infantile spasms, early onset epilepsy and hypsarrhythmia. Interestingly, several clinical studies strongly suggest that inactivation of *CDKL5* may be in part responsible for the occurrence of seizures symptoms. Thus it is tempting to speculate that there might be multiple targets of *CDKL5* that regulate different neurological activities including seizures³. Furthermore, while *MeCP2* is a nuclear protein, *CDKL5* shuttles between the nucleus and the cytoplasm, and has recently been found to be closely associated with nuclear speckles and involved in their structural organization^{6,14}. Interesting data have been obtained by Chen and colleagues in rat brain, indicating that *CDKL5* acts as a critical regulator of neuronal morphogenesis through a signalling pathway involving the Rac1 GTPase. These results suggest a possible cellular mechanism that might explain the disease phenotype observed in *CDKL5* patients¹⁵. Starting from these results and considering that the only substrate of *CDKL5* identified so far is

CDKL5 itself, the discovery and characterization of its substrates and interacting partners will contribute to gain new insights into the mechanisms underlying its function in neuronal development. We thus decided to perform gene expression profiling in iPSCs cells in order to identify the consequences of CDKL5 deficiency and with the idea to detect differentially expressed genes that might be involved both in neurogenetic processes and in common regulatory circuits with CDKL5, thus playing a possible role in the pathophysiology of CDKL5-related disorders. To this purpose we compared the global gene expression pattern at the transcript level in matched pairs of wild-type and mutant iPSCs clones from two different patients, a male with a missense mutation affecting the catalytic activity of the protein and a female with an early truncating mutation causing the loss of 2/3 of the protein.

3. RESULTS

Result 3.1

iPS cells for CDKL5-related disorders

Amenduni M, De Filippis R, Cheung AY, Disciglio V, Epistolato MC, Ariani F, Mari F,
Mencarelli MA, Hayek Y, Renieri A, Ellis J, Meloni I.

Eur J Hum Genet .2011 Jul 13. doi:10.1038/ejhg.2011.131. [Epub ahead of print]



ARTICLE

iPS cells to model CDKL5-related disorders

Mariangela Amenduni^{1,7}, Roberta De Filippis^{1,7}, Aaron YL Cheung², Vittoria Disciglio¹,
Maria Carmela Epistolato¹, Francesca Ariani¹, Francesca Mari^{1,3}, Maria Antonietta Mencarelli^{1,3},
Youssef Hayek⁴, Alessandra Renieri^{*,1,3}, James Ellis^{2,5,6} and Ilaria Meloni¹

Rett syndrome (RTT) is a progressive neurologic disorder representing one of the most common causes of mental retardation in females. To date mutations in three genes have been associated with this condition. Classic RTT is caused by mutations in the *MECP2* gene, whereas variants can be due to mutations in either *MECP2* or *FOXG1* or *CDKL5*. Mutations in *CDKL5* have been identified both in females with the early onset seizure variant of RTT and in males with X-linked epileptic encephalopathy. *CDKL5* is a kinase protein highly expressed in neurons, but its exact function inside the cell is unknown. To address this issue we established a human cellular model for *CDKL5*-related disease using the recently developed technology of induced pluripotent stem cells (iPSCs). iPSCs can be expanded indefinitely and differentiated *in vitro* into many different cell types, including neurons. These features make them the ideal tool to study disease mechanisms directly on the primarily affected neuronal cells. We derived iPSCs from fibroblasts of one female with p.Q347X and one male with p.T288I mutation, affected by early onset seizure variant and X-linked epileptic encephalopathy, respectively. We demonstrated that female *CDKL5*-mutated iPSCs maintain X-chromosome inactivation and clones express either the mutant *CDKL5* allele or the wild-type allele that serve as an ideal experimental control. Array CGH indicates normal isogenic molecular karyotypes without detection of *de novo* CNVs in the *CDKL5*-mutated iPSCs. Furthermore, the iPSC cells can be differentiated into neurons and are thus suitable to model disease pathogenesis *in vitro*.

European Journal of Human Genetics advance online publication, 13 July 2011; doi:10.1038/ejhg.2011.131

Keywords: CDKL5; Rett syndrome; induced pluripotent stem cells (iPSC); disease modelling

INTRODUCTION

Rett syndrome (RTT) is a progressive neurological disorder that affects 1 in 10 000 girls worldwide and represents one of the most common causes of mental retardation in females. RTT is characterized by an apparently normal development for the first 6–18 months of life, followed by regression with the onset of clinical signs including mental retardation, loss of speech, acquired microcephaly, growth retardation, autistic features, seizures, ataxia and hand stereotypies.¹ Beside the classic form, several RTT variants have been described including the Zappella variant, the congenital form, the ‘forme fruste’ and the early onset seizures variant.^{2–5} In past years, mutations in three genes have been associated with classic and/or variant RTT: *MECP2* and *CDKL5*, located on the X chromosome, and *FOXG1*, on chromosome 14.^{1,6,7} About 80% of classic RTT cases are caused by mutations in *MECP2* that encodes for a methyl-CpG-binding protein involved in the regulation of gene expression.^{8,9} To investigate the molecular mechanisms leading from *MECP2* mutations to RTT onset, different mouse models have been generated and extensively characterized.^{10–13} These models allowed identification of specific alterations in glutamatergic neurons:¹³ cells lacking *Mecp2* have reduced synapse numbers and, accordingly, they show a reduced synaptic response. The opposite effects are elicited by *Mecp2* over-expression. In spite of these important breakthroughs on the pathophysiology of RTT in animal models, the inaccessibility of the main affected human tissue and the

impossibility of establishing good *in vitro* human cellular models have greatly complicated research efforts. In this respect, the development in 2007 of induced pluripotent stem cells (iPSCs) offered an unprecedented opportunity for the creation of patient- and disease-specific human cellular models. In fact, iPSCs can be obtained from differentiated somatic cells, for example fibroblasts, through the induction of expression of a few transcription factors related to pluripotency, usually OCT-4, SOX-2, c-MYC and KLF-4.¹⁴ iPSCs are similar to human embryonic stem cells (hESCs) in morphology, proliferation, gene expression and *in vitro* differentiation potential. Like hESCs, they can be expanded indefinitely and differentiated *in vitro* into many different cell types.¹⁴ These features make them the ideal tool to study disease mechanisms directly on the primarily affected cells. Up to now, iPSCs have been successfully derived from patients with both neurodegenerative (ALS, SMA, Parkinson, HD, FD) and neurodevelopmental (FRAXA, PW-AS) disorders, and neuronal differentiation has been performed in some cases, using protocols developed for hESCs.^{15–17} Interestingly, a consistent neuronal phenotype was observed for SMA and FD, confirming the potential of this technology to model neurological disorders.¹⁵ Very recently, Marchetto *et al.*¹⁸ applied this technology to model RTT *in vitro*. In fact they derived iPSCs from *MECP2*-mutated patients fibroblasts and differentiated them into glutamatergic neurons. They found that RTT neurons have a reduced number of dendritic spines compared with those derived from control

¹Medical Genetics, Department of Biotechnology, University of Siena, Siena, Italy; ²Developmental & Stem Cell Biology Program, SickKids, Toronto, Ontario, Canada; ³Medical Genetics, Azienda Ospedaliera Universitaria Senese, Siena, Italy; ⁴Child Neuropsychiatry, University hospital of Siena, Siena, Italy; ⁵Ontario Human iPSC Cell Facility, SickKids, Toronto, Ontario, Canada; ⁶Department of Molecular Genetics, University of Toronto, Toronto, Ontario, Canada

*Correspondence: Professor A Renieri, Medical Genetics, Department of Biotechnology, University of Siena, Policlinico S. Maria alle Scotte, viale Bracci 2, 53100 Siena, Italy. Tel: +39 0577 233303; Fax: +39 0577 233325; E-mail: renieri@unisi.it

⁷These authors contributed equally to this work.

Received 31 December 2010; revised 15 April 2011; accepted 3 June 2011

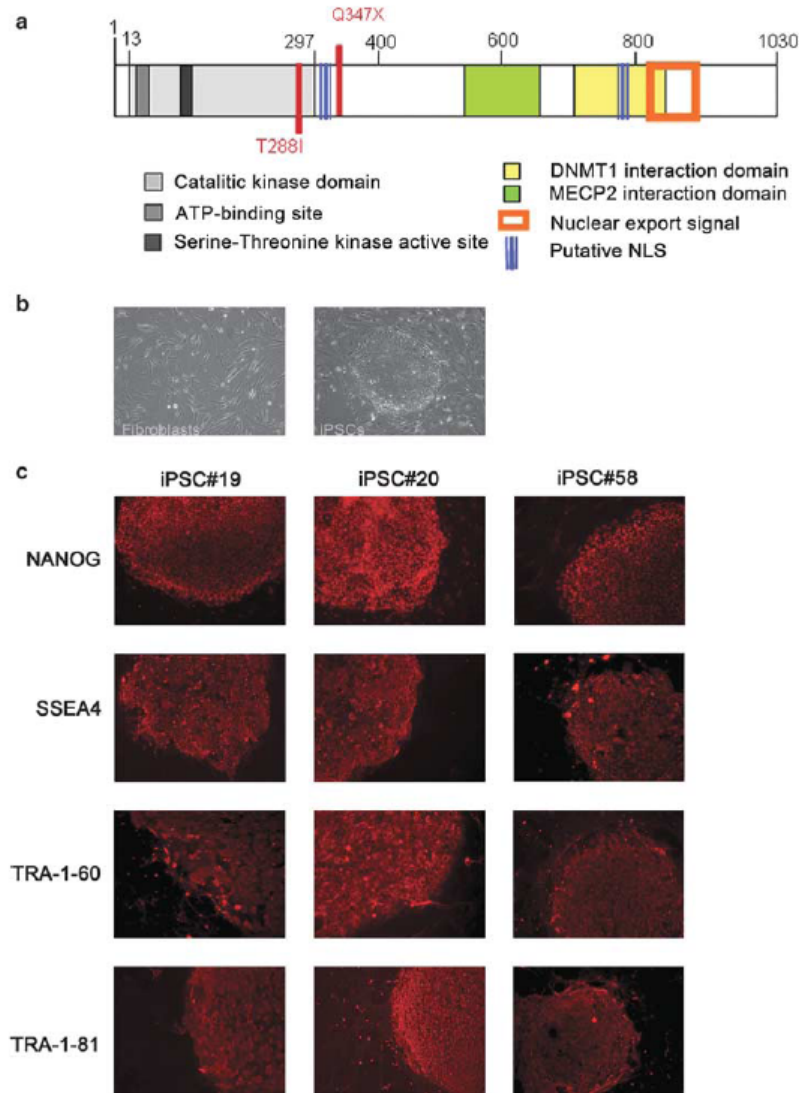


Figure 1 Generation and characterization of iPSCs. (a) Schematic representation of CDKL5 protein structure with the known functional domains. The mutations identified in the patients reported in this study are shown in red. (b) Phase contrast image of human fibroblasts morphology before reprogramming (left) and typical morphology of one iPSC clone (right). Cells surrounding the clone are mitomycin-C-inactivated mouse embryo fibroblasts (feeders). (c) Representative images of immunostaining for pluripotency markers for two clones derived from patient 1 (iPSC #19 and iPSC#20) and one clone from patient 2 (iPSC #58). Images are at $\times 20$ magnification.

iPSCs or hESCs. Moreover, they also demonstrated an important reduction in the frequency and amplitude of spontaneous excitatory and inhibitory postsynaptic currents in RTT neurons. It is important to underline that these findings are in accordance with the data on mouse models and thus demonstrate the applicability of iPSCs technology to model RTT *in vitro*.

Unlike the classic form, RTT variants are mainly due to mutations in the other two genes, *CDKL5* and *FOXG1*. In particular, mutations in *CDKL5* have been identified in the early onset seizures variant of RTT in females and in X-linked epileptic encephalopathy in males.^{19,20} *CDKL5* is a kinase protein that shuttles between the cytoplasm and the

nucleus (Figure 1a).²⁰ A direct interaction with MeCP2 has been demonstrated, in accordance with their common involvement in RTT: *CDKL5* can bind and phosphorylate MeCP2 *in vitro*, and MeCP2 in turn regulates *CDKL5* gene expression, at least in certain brain regions.^{19,21,22} Moreover, the two proteins bind to different regions of DNMT1 further suggesting the possibility of a participation in common pathways.²³ Intriguingly, *CDKL5* shows high expression levels in neurons but it is undetectable in glial cells, indicating an important role in neuronal development and/or function.²⁰ A mouse model for *CDKL5*-related disease is currently lacking, limiting our knowledge of the function of *CDKL5* inside the neuron. Recently,

Chen *et al*²⁴ gave us a first glimpse by using RNA interference to silence *Cdkl5* expression in rat cortical neurons. They demonstrated that *Cdkl5* is essential for neuronal morphogenesis as its downregulation in cultured neurons inhibits neurite outgrowth and dendritic arborization whereas its over-expression elicits the opposite effect. At present it is not clear whether these findings recapitulate the situation in affected human brain. To answer this question, we have reprogrammed fibroblasts from patients carrying different *CDKL5* mutations into iPSCs with the aim of establishing a human neuronal model for *CDKL5*-associated disease. We report here that female *CDKL5*-mutated iPSCs maintain X-chromosome inactivation, have normal molecular karyotype indicating that they are isogenic, and we identify clones expressing either the wild-type or the mutant *CDKL5* allele. We show that the cells can be differentiated into neurons and are thus suitable to model disease pathogenesis.

METHODS

Fibroblasts reprogramming and hiPSCs culture

Following informed consent signature, skin biopsies (about 3–4 mm²) were performed using the Punch Biopsy procedure. Fibroblasts were isolated and cultured with standard protocols.²⁵ Fibroblasts at passage 2 or 3 were reprogrammed following the protocol by Hotta *et al*²⁶ that allows to enrich for reprogrammed cells. Briefly, fibroblasts were first infected with a lentiviral vector to stably introduce a reporter gene (EGFP) and a puromycin resistance gene under the control of an hESCs-specific promoter; parallel infection with a second lentivirus encoding the mouse mSlc7a1 receptor allowed the subsequent use of mouse-specific retroviruses for the expression of the reprogramming factors (OCT-4, SOX-2, c-MYC and KLF-4), reducing the risks of infection for operators. Seven days after retrovirus infection, fibroblasts were passed onto mitomycin-C-inactivated mouse embryo fibroblasts (feeders) and puromycin selection (0.8 µg/ml) (Invitrogen, Milan, Italy) was started on day 21 to selectively kill non-reprogrammed cells. Emerging iPSCs colonies were manually picked and expanded on feeders for some passages. Established clones that maintained a good hESCs-like morphology were moved to feeders-free culture conditions on Matrigel-coated dishes (BD Biosciences, Milano, Italy) in mTeSR1 medium (Stem Cell Technologies, Grenoble, France) with puromycin. From this point, cells were routinely passed by Collagenase IV treatment (Invitrogen).

Clones characterization

Genotyping. DNA from parental fibroblasts and iPSC clones was extracted with QIamp DNA mini kit (Qiagen, Milan, Italy) according to manufacturer's protocol. One hundred nanograms of DNA were PCR amplified using standard conditions and sequenced with the BigDye Terminator v1.1 Cycle Sequencing kit (Applied Biosystems, Milan, Italy) following manufacturer's protocol. Intronic primers flanking the exons harboring the mutations were used for both PCR and sequencing.

Immunostaining. Cells grown on coverslips were fixed with 4% paraformaldehyde in 1× PBS for 10 min at 37°C and permeabilized with 1× PBS/0.01% Triton X-100 for 10 min at RT. Two hours incubation with blocking buffer (6% NGS, 0.5% BSA in PBS-T) at RT was performed. Subsequently, cells were incubated with appropriate dilutions of primary antibodies in blocking buffer O/N at 4°C. The next day, cells were washed three times with 1× PBS-T (0.1% Tween20 in 1× PBS) and then incubated for 1 h with the secondary antibodies in blocking buffer. Finally, cells were washed three times with 1× PBS-T, stained with DAPI 1 µg/ml in 1× PBS for 10 min. Coverslips were mounted with Mowiol and observed with a Axioscop 40FL (Zeiss, Milan, Italy) microscope connected to a computer. Images were merged and analyzed using ImageJ. Antibodies for the following hESCs-specific markers were used: NANOG (R&D, Minneapolis, MN, USA), SSEA3 (Invitrogen), SSEA4 (Invitrogen), TRA-1-60 (Invitrogen), TRA-1-81 (Invitrogen).

In vitro differentiation via embryoid bodies formation. Cells were harvested by collagenase treatment and clumps were transferred on two wells of low-cluster 6-wells plates with embryoid bodies (EBs) medium (knockout

D-MEM supplemented with 10% FBS, 2 mM L-Glutamine, 50 U/ml penicillin, 50 mg/ml streptomycin, 0.1 mM non-essential amino acids and 0.5 mM β-mercaptoethanol) and allowed to grow in suspension for 8 days. The resulting EBs were plated on collagen-coated coverslips (0.05 mg/ml collagen acetic acid 0.1% in H₂O) and allowed to grow for another 8 days. The presence of differentiated cells of all three germ layers was tested by immunostaining (protocol described above) for lineage-specific markers: β-III-tubulin (Chemicon, Milan, Italy) for ectoderm, GATA-4 (Santa Cruz Biotechnologies, Heidelberg, Germany) for endoderm and smooth muscle actin (SMA; Invitrogen) for mesoderm.

Real-Time qPCR. Total RNA from iPSC clones was isolated with Trizol reagent (Invitrogen). One microgram of total RNA was reverse transcribed with high-capacity cDNA reverse transcription kit (Applied Biosystems) according to manufacturer's instructions. Primer sets that allow the selective amplification of either the transgenes (OCT4, SOX2, KLF4 and C-MYC) or their endogenous counterparts were employed. Glyceraldehyde-3-phosphate dehydrogenase or actin were used as reference genes. PCR was carried out in single-plex reactions in a 96-well optical plate with FastStart SYBR Green Master Mix (Roche, Milan, Italy) on an ABI Prism 7700 Sequence Detection System (Applied Biosystems). Experiments were performed in triplicate in a final volume of 20 µl with 5 ng of cDNA and 150 nM of each primer, following SYBR Green protocol. Standard thermal cycling conditions were employed (Applied Biosystems): 2 min at 50°C and 10 min at 95°C followed by 40 cycles at 95°C for 15 s and 60°C for 1 min. Results were analyzed using the comparative Ct method.

Molecular karyotyping by array-CGH. Array-CGH analysis was carried out on DNA extracted from clones at passage 15 or later using commercially available oligonucleotide microarrays with an estimated average spatial resolution of ~45 kb (Human Genome CGH Microarray 44B Kit; Agilent Technologies, Milan, Italy) as previously reported (Sampieri K Cancer Sci 2009). Image analysis was carried out using CGH Analytics Software v. 3.4.40 (Agilent Technologies) with default settings. DNA from parental fibroblasts was also analyzed to identify constitutional CNVs.

X-inactivation analysis

The X-inactivation status was estimated using an assay based on a methylation-sensitive HpaII restriction site located in the androgen receptor gene.²⁷ This site is methylated on the inactive X, and unmethylated on the active X chromosome. A polymorphic CAG repeat located within the amplified region is used to distinguish the two alleles. Genomic DNA from iPSCs and parental fibroblasts was digested with HpaII enzyme O/N at 37°C. For each sample two separate PCR reactions, on digested and undigested DNA, were performed using a fluorescent-dye-labelled primer set (Applied Biosystems). PCR products were run on an ABIPRISM GA3130 sequencer and analyzed with Gene Mapper software (Applied Biosystems). To estimate fragments length, FAM-labelled products were simultaneously compared with a LIZ size standard. PCR products from digested and undigested DNA were compared to estimate the X-chromosome inactivation (XCI) status.

Neuronal differentiation

The experiment was performed on two clones from patient 1 (iPSC#19 expressing mutant *CDKL5* allele and iPSC#20 expressing wild-type *CDKL5*) and a normal male control iPSC clone derived from a newborn male BJ fibroblast line (cell line no CRL-2522) obtained from ATCC.²⁶ Neuronal differentiation was performed following a protocol established for human ESCs.^{28,29} Briefly, cells were allowed to grow as EBs for 4 days in human ES medium (knockout DMEM supplemented with 15% KO serum replacement, 2 mM L-glutamine, 50 U/ml penicillin, 50 mg/ml streptomycin, 0.1 mM non-essential amino acids and 0.5 mM β-mercaptoethanol) and for 2 additional days in neuronal medium (DMEM/F12 supplemented with 1× N2, 0.1 mM non-essential amino acids and 2 µg/ml Heparin). At day 6, cells were plated onto laminin-coated plates and allowed to grow for 9 additional days. In this period neural precursor cells organized in neural rosettes emerged. The propensity of cells to differentiate toward the neuronal lineage was determined by calculating the percentage of plated EBs that formed neural rosettes. Rosettes were then manually lifted and allowed to grow as floating neurospheres for some days in neuronal medium

plus 1× B27 supplement. Finally, neurospheres were plated onto poly-N-oronithine and laminin-coated slides or plates for final differentiation.

Based on data on human ESCs, the protocol is expected to originate mainly glutamatergic neurons.^{28,29} To confirm the identity of the obtained neurons, immunofluorescence was performed as described above using markers for both glutamatergic and GABAergic neurons: VGLUT1 (Invitrogen) and GAD65/67 (Chemicon). The generic neuronal markers β -III-tubulin or MAP2 (Abcam, Cambridge, UK) were used for neurons visualization. In addition, RT-PCR analysis was performed for the expression of markers of glutamatergic (VGLUT1, VGLUT2 and TBR1) and GABAergic (GAD67) neurons as well as glial cells (GFAP). Primer sequences are reported in Supplementary Table 1. Finally, in order to compare the efficiency of differentiation into glutamatergic and GABAergic neurons between different clones, real-time quantitative RT-PCR experiments were performed using commercial TaqMan probes (VGLUT1 assay id: Hs00220404_m1; GAD67 assay id: Hs01065893_m1) on an ABI Prism 7700 Sequence Detection System. The glyceraldehyde-3-phosphate dehydrogenase gene was used as a reference (Applied Biosystems). Experiments were performed and analyzed as previously described.³⁰ The Student's *t*-test with a significance level of 95% was used for the identification of statistically significant differences in expression levels among different clones.

RESULTS

Patients selection

Patient 1 (no. 1567) is a 2-year-old girl with a clinical diagnosis of early onset seizures variant of RTT who started presenting epilepsy not controlled by therapy at 1 month of age. At present she is not able to walk and she does not speak. Hand stereotypies, esophageal reflux, constipation, sleep disturbances are present. She also shows normal head circumference, poor visual contact and social interaction. Detailed clinical information has been already reported³¹ (Patient 1).

Patient 2 (no. 1559) is a 9-year-old boy with normal development in the first 16 months of life. At the age of 8 months, the first epileptic fits appeared and later on he showed developmental arrest and language regression. At 13 months he was able to say several words; however, at present he is only able to utter a few disyllabic words. He can walk without assistance and presently he shows four to six epileptic episodes a day without any clinical amelioration by pharmacological treatment. He also presents cold feet, constipation and normal head circumference. No hand stereotypies are referred. Detailed clinical information is reported in Elia *et al*³² (Patient 2).

The two patients present different *CDKL5* mutations (Figure 1a): patient 1 has a truncating mutation (p.Q347X) resulting in a protein lacking 2/3 of its amino acids, including the domains responsible for the interaction with MeCP2 and DNMT1, and the nuclear export signal; patient 2 has a missense change (p.T288I) affecting a highly conserved amino acid inside the catalytic kinase domain. Patient fibroblasts were obtained from the 'Cell lines and DNA bank of Rett Syndrome and other X-linked mental retardation' biobank.

Generation and Characterization of iPS cells

Patient fibroblasts at low passage number were reprogrammed using a published protocol.^{14,26} Two weeks after infection with the reprogramming transgenes, the first morphological changes were visible, and compact iPSC-like colonies were identified 1–2 weeks later. At least 25 colonies for each patient were picked and expanded (Figure 1b). Three clones from patient 1 and five from patient 2 were selected for further characterization. Direct sequencing of the *CDKL5* genomic region confirmed that iPSCs contained the expected mutation and thus were derived from the respective patient fibroblasts (data not shown). Standard tests were performed to confirm the fully reprogrammed status of the selected clones. All clones had a typical hESC-like morphology and expressed hESC-specific antigens such as NANOG, SSEA3, SSEA4, TRA-1-60 and TRA-1-81 (Figure 1c). Quantitative

RT-PCR experiments demonstrated that all but one clone silenced the four retroviral transgenes (OCT4, SOX2, KLF4, c-MYC) and reactivated the corresponding endogenous genes at levels comparable to those of hESCs (Figures 2a and b). The clone derived from patient 2 that retained partial transgene expression was excluded from further analyses. *In vitro* differentiation via embryoid body formation confirmed the ability of the clones to spontaneously differentiate into cells of the three germ layers (Figures 2d and e). Molecular karyotyping was performed by array-CGH to test whether the clones retained a normal karyotype. The same analysis was performed also on parental fibroblasts, to identify constitutive CNVs already present in the patients. All three clones deriving from patient 1 had a normal 46XX karyotype (Figure 2c and Supplementary Figure 1A). A polymorphic duplication in Xq22.2 was identified in the three clones, as well as in the parental fibroblasts (Supplementary Figure 1A). Of the four clones from patient 2 that passed previous characterization steps, a normal 46XY karyotype was found in three. Analysis of the fourth clone (iPSC #52) revealed a trisomy of chromosome 8 (Supplementary Figure 1B) and this line was not studied further. These data indicate that no detectable *de novo* CNVs arose during reprogramming and that the cells are isogenic.

X-inactivation analysis

As *CDKL5* is an X-linked gene, we decided to test whether in female iPSCs X-inactivation was maintained or erased. To this aim we used the standard androgen-receptor gene test.²⁷ The assay was initially performed on the three characterized clones and demonstrated that all had retained XCI and consistently showed only one active X chromosome (Figure 3a). We thus extended the analysis to three additional clones derived from the same patient. In all three clones, the analysis demonstrated the presence of only one active X chromosome (Table 1). Interestingly, we identified clones deriving from the same patient but with different inactive X chromosomes (Figure 3a). These results suggested that they might express either the wild-type or the mutated *CDKL5* allele. To confirm this hypothesis we sequenced *CDKL5* mRNA (Figure 3b). As expected, parental fibroblasts showed expression of both alleles, consistent with random X inactivation. On the contrary, the iPSC clones exclusively expressed only one allele; in accordance with results of XCI analysis, one clone expressed the wild-type *CDKL5* allele, whereas the others expressed the mutated allele (Figure 3b and data not shown). To confirm that this situation was stably maintained upon cell expansion in culture, XCI analysis was performed on cells at later passages for the two clones that were selected for further experiments (iPSC #19 and #20). The initial analysis had been performed on cells at passage 29 (clone #19) and 21 (clone #20). We thus analyzed cells at passages 32 and 41 for clone #19 and 23, and 32 for clone #20. For both clones, cells at later passages retained XCI (Table 1).

Neuronal differentiation

To confirm that cells were suitable as an *in vitro* model to study the pathogenesis of *CDKL5*-related disorders, we induced the iPSCs toward a neuronal fate.^{28,29} In order to avoid confounding effects due to differences in genetic background, we decided to concentrate our attention on the two clones from patient 1 that are genotypically identical but differ for *CDKL5* expression (iPSC #19 expressing mutant *CDKL5* allele and iPSC #20 expressing wild-type *CDKL5*). BJ-iPSC clone derived from a normal male individual was included as a control for the differentiation process. Visual examination of cells all along the differentiation process suggested that our clones differentiated following the expected course (Figures 4a–f). Neural rosettes

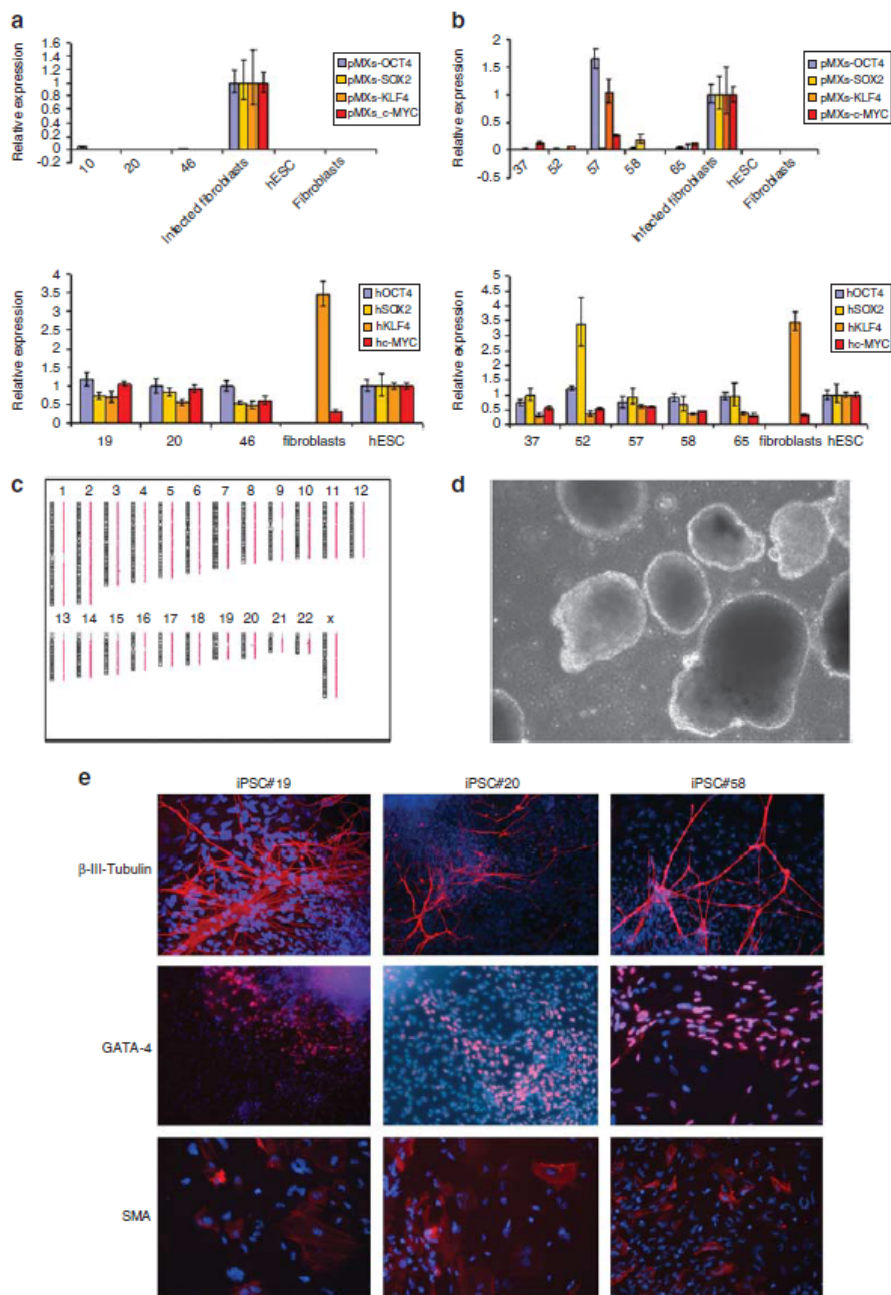


Figure 2 iPSCs characterization. (a, b). Summary of real-time RT-PCR experiments demonstrating that clones derived from patient 1 (a) and from patient 2 (b) have inactivated the four transgenes (upper panel in a, b) and reactivated the corresponding endogenous genes (lower panel). A human ESC line and freshly infected fibroblasts were used as positive controls for the expression of endogenous genes and transgenes, respectively. Parental fibroblasts were also analyzed. Clone #57 from patient 2 maintained transgenes expression and it was thus excluded from further experiments. (c) Representative array CGH result from iPSC #19 from patient 1 showing a normal karyotype. (d) Phase contrast image of EBs after 5 days of suspension culture. (e) Immunostaining of EBs after 16 days of differentiation shows staining for markers specific of all three germ layers: β -III-tubulin (ectoderm), GATA-4 (endoderm) and smooth muscle actin (SMA; mesoderm). Representative images of two clones from patient 1 (iPSC #19 and iPSC #20) and one clone from patient 2 (iPSC #58) are shown. Images are at $\times 20$ magnification.

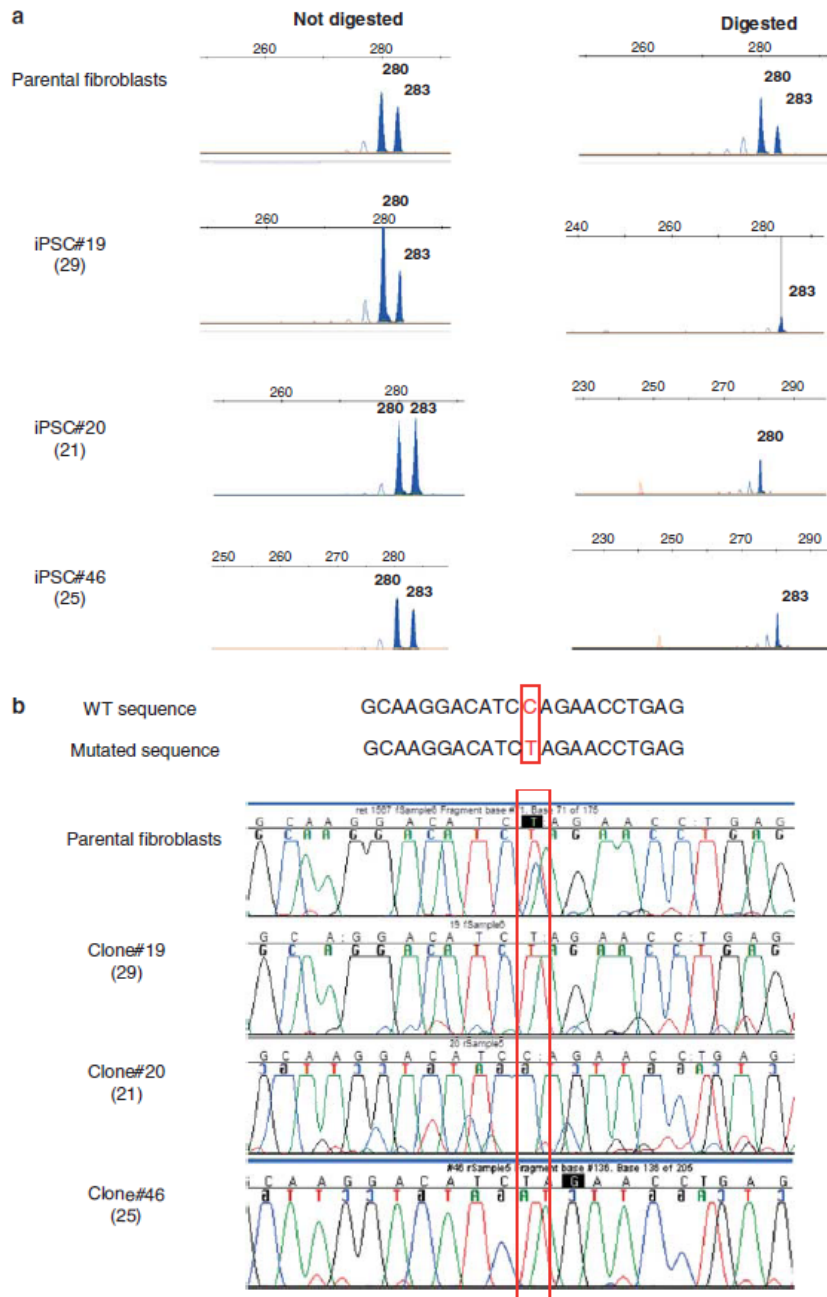


Figure 3 X-inactivation analysis. (a) In parental fibroblasts two alleles can be identified. PCR on digested DNA still result in two peaks, indicating a balanced XCI pattern. Undigested DNA from the three iPSC clones (#19, #20 and #46) present the same two peaks observed in parental fibroblasts. However, following digestion, each clone present only one peak, indicating a skewed pattern of XCI. Comparison of alleles length demonstrates that the three clones inactivate different X chromosomes. (b) Direct sequencing on cDNA from parental fibroblasts and iPSCs clones #19, #20 and #46 from patient 1. Wild-type and mutated sequences are shown at the top with the mutated nucleotide outlined in red. The chromatograms show that RNA isolated from parental fibroblasts presents both alleles whereas iPSCs clones express only one allele (mutated nucleotide outlined by a red rectangle). In particular, clones #19 and #46 express the mutated *CDKL5* allele whereas clone #20 expresses the wt (wild-type) allele. Passage number at the moment of DNA and RNA extraction is indicated in parenthesis below clone number.

Table 1 XCI analysis

Sample	Passage no.	X-inactivation status	Size of inactive allele ^a (bp)
iPSC #19	32	Skewed	283
iPSC #19	41	Skewed	283
iPSC #20	23	Skewed	280
iPSC #20	32	Skewed	280
iPSC #33	13	Skewed	283
iPSC #48	16	Skewed	283
iPSC #60	24	Skewed	283

Abbreviations: iPSC, induced pluripotent stem cell; XCI, X-chromosome inactivation.

^aThe inactive allele corresponds to the one that is amplified also after *HpaII* digestion due to methylation of the enzyme-recognition sequence.

consisting of one or more layers of columnar cells arranged in a tubular structure were visible in all clones a few days after EBs seeding (Figure 4a). Shortly after plating the neurospheres for final differentiation, numerous cell processes started to emerge from the spheres giving them a star-like appearance (Figure 4b). When allowed to differentiate further, cell processes formed bundles of fibers and cells could be seen migrating away from the spheres (Figures 4c and d). At this stage, MAP2-positive neurons could be identified for all clones (Figures 4e and f). Based on data on human ES, the protocol was expected to originate mainly glutamatergic neurons.^{28,29} To determine whether this was indeed the case, cells were differentiated for 10 weeks and mature neurons were analyzed. RT-PCR with primers for glutamatergic (VGLUT1, VGLUT2 and TBR1) and GABAergic (GAD67) neurons demonstrated that the cultures contained both neuronal types (Figure 4j). GFAP-positive glial cells were also present (Figure 4j). This result was confirmed by immunostaining for VGLUT1 and GAD65/67. In particular, our data indicate that, as expected, the majority of the resulting neurons are glutamatergic but GABAergic neurons are also present (Figures 4g and h). Mature cultures also contained many non-neuronal cells that were negative for both MAP2 and β -III-tubulin staining (Figure 4i).

In order to obtain a first estimate of the ability of our clones to differentiate toward a neuronal fate, the percentage of seeded EBs that formed clearly identifiable rosette structures on day 15 was calculated (Figure 4k). The analysis was performed on two independent experiments, with comparable results. The clones formed rosettes with efficiency ranging from 37% in the BJ-iPS to 47% in clone #19. Interestingly, the two clones derived from patient 1 (iPSC #19 and #20) displayed very similar efficiencies (47% and 46%, respectively) (Figure 4k). We then decided to evaluate whether the different clones formed glutamatergic and GABAergic neurons with the same efficiency. No gross differences were visible but the high density of the neuronal network arising in culture did not allow us to calculate the percentage of cells in the two populations from immunofluorescence images. As a consequence, to evaluate differences in the potential of single clones to differentiate into glutamatergic or GABAergic neurons, real-time quantitative RT-PCR was performed on RNA extracted from 10-week-old neurons using probes for VGLUT1 or GAD67, respectively (Figure 4l). Our results showed that the three analyzed clones differed significantly from each other for VGLUT1 expression, with the highest expression in iPSC #20. GAD67 expression was comparable between iPSC #19 and the normal control clone, whereas iPSC #20 again showed significantly higher expression.

DISCUSSION

RTT is one of the most common causes of mental retardation in females. In spite of intense research efforts, clarification of the molecular mechanisms of RTT, as well as all other neurologic disorders, has been hampered by the lack of satisfactory human *in vitro* cellular models. Mouse models represent a useful alternative to mimic human monogenic neurological disorders and they have allowed important insights into disease mechanisms of RTT due to *MECP2* mutations. However, mouse models often do not faithfully recapitulate human conditions and they do not take into account the influence of genetic background on disease phenotype. In this respect, an unprecedented opportunity for the creation of patient- and disease-specific human cellular models is represented by iPSCs.¹⁵ Very recently iPSCs technology has been applied to model RTT starting from fibroblasts of *MECP2*-mutated patients.¹⁸ *MECP2* is the most commonly mutated gene in classic RTT, and it has thus been the most extensively studied. Less is known about *CDKL5*, the gene associated to the early onset seizures variant of RTT and to other forms of X-linked intellectual disabilities.^{19,20} In order to clarify the role of *CDKL5* in human affected neurons, we used iPSC technology to establish a human cellular model that recapitulates *CDKL5*-related disorders. To this aim, we reprogrammed fibroblasts from a hemizygous male with a missense mutation affecting an highly conserved residue inside the catalytic kinase domain, and a heterozygous female with a stop mutation downstream of the kinase domain predicted to result in a truncated protein lacking 2/3 of its amino acids.^{31,32} Fibroblasts from both patients were successfully reprogrammed. iPSCs lacking a functional *CDKL5* protein (those derived from the hemizygous male patient and those deriving from the female but expressing only mutant *CDKL5*) did not show obvious differences in proliferation with respect to the clone expressing wild-type allele or to BJ-iPS and could be easily passaged several times (at least 25 passages) without any apparent change.

Recent studies report that the reprogramming process is associated with accumulation of *de novo* CNVs, especially in early passage iPSCs.^{33,34} We thus decided to perform array-CGH analysis in our pluripotent clones in order to more accurately check for the presence of imbalances deriving from the reprogramming process. Among the seven clones that we analyzed (three from patient 1 and 4 from patient 2), only one presented a trisomy of chromosome 8 and was not studied further, while the others did not show any obvious alteration (Figure 2c and Supplementary Figure 1). Although our CNV detection method is less sensitive than previous studies (75 kb compared with 30 kb), our results from clones at passages higher than 15 are consistent with the report by Hussein *et al* that *de novo* CNVs are selected against during expansion in culture. Thus, the iPSC cell clones we derived are isogenic and display a normal molecular karyotype at this resolution.

In order to allow dosage-compensation for genes on the X chromosome between males and females, in mammalian female cells one of the two X chromosomes is silenced early during development through a mechanism defined as XCI.³⁵ In accordance with their derivation from the inner cell mass of the blastocyst, at a pre-XCI stage, female mouse ESCs carry two active X chromosomes that undergo random XCI upon differentiation.³⁶ The same situation is observed in mouse iPSCs.³⁷ Human ESCs reveal a heterogeneous status: most undifferentiated hESC lines carry an inactive X chromosome, but some sublines containing two active X chromosomes can be identified.³⁸ XCI status in human iPSCs is still controversial. In fact, it has been demonstrated that Duchenne muscular dystrophy and *MECP2*-null iPSC cells retain an inactive X chromosome in a clonal pattern with one

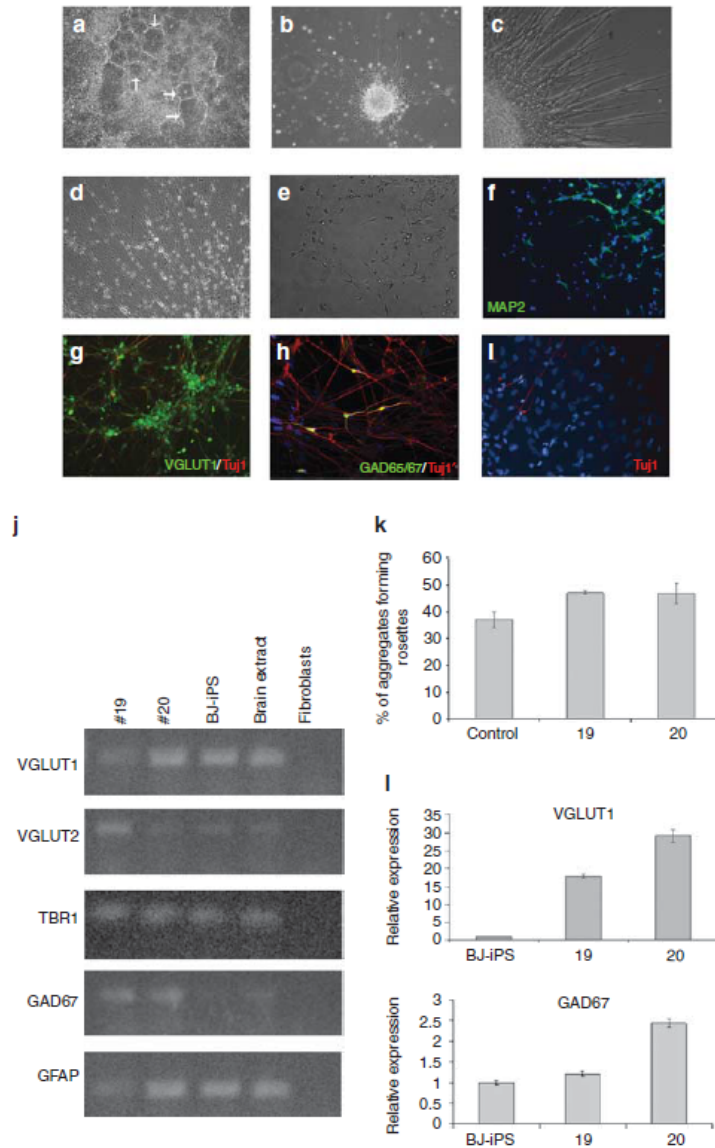


Figure 4 *CDKL5*-mutated iPSCs differentiate into neurons. iPSCs were induced to differentiate into neurons following a published protocol. (a) Neural rosettes (arrows) consisting of columnar cells arranged in a tubular structure were visible a few days after EBs seeding. (b) Shortly after neurospheres plating, numerous cell processes started to emerge from the spheres giving them a star-like appearance. (c, d) When cells were allowed to differentiate further, cell processes formed bundles of fibers (c) and cells could be seen migrating away from the spheres (d). (e, f) At this stage MAP2-positive neurons (green in f) could be identified by immunofluorescence. (g, h) After 10 weeks of differentiation the majority of β -III-tubulin-positive neurons (Tuj1, red) were also positive for VGLUT1 (green in g), but cells positive for the GABAergic marker GAD65/67 could be also identified (green in h). (i) In addition to neurons, many β -III-tubulin-negative non-neuronal cells were present in our cultures, as evidenced by DAPI-positive nuclei (blue). Images are at $\times 20$ magnification. Blue staining=DAPI. (j) RT-PCR analysis on RNA isolated from 10-week-old neuronal cultures demonstrates that glutamatergic (VGLUT1, VGLUT2, TBR1) and GABAergic (GAD67) neurons, and glial cells (GFAP) are present in our cultures. RNA isolated from parental fibroblasts was used as negative control; a commercial RNA from human total brain was used as positive control. (k) The ability of our cells to differentiate toward a neuronal fate was estimated as the percentage of plated EBs that formed rosettes on day 15. Histograms represent the mean of two independent experiments. Error bars represent standard deviation. (l) Results of quantitative real-time RT-PCR on neuronal cultures show a high variability of expression of both VGLUT1 (upper panel; $P < 0.0001$) and GAD67 (lower panel; $P < 0.0001$ between BJ-iPS and #20, and between #19 and #20; $P < 0.05$ between BJ-iPS and #19) in the three clones. Expression in neurons derived from the normal control clone was arbitrarily set as 1. Error bars represent standard deviation from three replicates of each sample.

of the two X chromosomes exclusively inactivated in all the cells of a single clone.^{39,40} However, Marchetto *et al*¹⁸ recently reported that X inactivation can also be erased during reprogramming of hiPSCs and it is subsequently restored upon differentiation. Considering this controversy and as *CDKL5* is an X-linked gene that when mutated causes RTT like *MECP2*, we tested XCI in our female iPSCs clones from patient 1. In accordance with the data reported by Tchieu *et al* and Cheung *et al* our clones present XCI. Interestingly, while parental fibroblasts show random XCI, each clone exclusively expresses one of the two X chromosomes (Figure 3 and Table 1). Moreover, analysis of the same clones at different passage numbers indicated that they stably maintained exclusive expression of the same X chromosome upon expansion in culture (Table 1). The clonal nature of XCI in our clones and in those reported by Tchieu³⁹ and by Cheung⁴⁰ confirm the hypothesis that in human cells XCI is usually not erased during reprogramming, but each iPSC clone maintains the same inactive X chromosome as the original reprogrammed fibroblast from which it was derived.³⁹ Apart from the general relevance to our understanding of the reprogramming process, the finding that hiPSCs retain XCI has important implications also for the application of these cells for *in vitro* modelling of X-linked disorders. In fact, it implies that from female fibroblasts with random XCI, it is possible to obtain iPSCs expressing either the mutant or wild-type allele of an X-linked gene.³⁹ This is in fact what we found for hiPSCs derived from the female patient (Figure 3). The clone expressing the WT allele is genetically identical to those expressing the mutated one; it thus represents the ideal isogenic control to test the effects of a mutation without the potentially confounding effect of genetic background.

To test whether our *CDKL5*-mutated hiPSCs could be used to model disease pathogenesis *in vitro*, we differentiated them into neurons following a protocol established for hESCs.^{28,29,41} The characterization of the neuronal differentiation process indicates that the cells can be differentiated into neurons and that the differentiation follows the stages observed in hESCs (Figures 4a–f).⁴¹ The clones show a variable but reproducible efficiency of differentiation toward the neuronal lineage, as already reported for iPSCs (Figure 4k).⁴² Interestingly, the two clones derived from patient 1 but expressing different *CDKL5* alleles (iPSC#19 and iPSC#20) have similar efficiencies, suggesting that the absence of a functional *CDKL5* protein does not affect the initial commitment toward a neuronal fate.

Based on data on hESCs, we expect the resulting cells to be mainly excitatory glutamatergic neurons.^{29,41} Immunofluorescence analysis with specific markers indicates that this is indeed the case, even though GABAergic neurons can be also identified (Figures 4g and h). The very dense network of cells in mature cultures did not allow us to directly estimate the relative percentages of neurons in the two populations. We thus decided to compare the ability of different clones to give rise to glutamatergic and GABAergic neurons by estimating the amount of VGLUT1 or GAD67 mRNA in mature cultures. We found very different expression levels for the two markers between the three analyzed clones (Figure 4l). In particular, for VGLUT1 the difference is statistically significant both between iPSC#19, expressing mutant *CDKL5*, and the other two clones, and between these last two clones that both express wild-type *CDKL5* (iPSC#20 and the control clone). Moreover, the difference is higher between these last two clones than with iPSC#19. This suggested that the observed difference is not a specific consequence of *CDKL5* absence but rather reflects clone-to-clone variability. For GAD67, iPSC#19 and the control clone present similar expression, but iPSC#20 has a statistically higher expression. This high variability was unexpected, as the evaluation of the ability of the clones to form

neural rosettes did not show dramatic differences between the three clones. To try to understand the reasons for these differences we thus examined our immunofluorescence slides. The mature cultures contained many non-neuronal cells that were negative for both MAP2 and β -III-tubulin staining. This is in accordance with other reports that indicate that a percentage of non-neuronal cells remain in the cultures.^{43,44} In particular, although an accurate quantitation could not be performed, cultures deriving from the BJ-iPS clone seem to have a higher number of non-neuronal cells compared with the other two clones. As this clone showed lowest expression of both VGLUT1 and GAD67, this finding suggests that heterogeneity of the neuronal cultures might be explained at least in part by the variable presence of non-neuronal cells. An alternative hypothesis is the presence of variable percentages of other neuronal types. Although we cannot presently confirm or exclude this hypothesis, the fact that the cells follow the expected differentiation course point to the presence of non-neuronal cells as the factor responsible for the apparent variability of VGLUT1 and GAD67 expression. It will be thus essential to develop accurate methods to enrich for neuronal precursors in order to have pure populations amenable to quantitative analyses.⁴³

The protocol we employed gives rise mainly to excitatory glutamatergic neurons.^{29,41} However, Li *et al*²⁹ reported that neural precursors can be redirected to form inhibitory GABAergic neurons by inhibition of Wnt pathway and/or activation of SHH. This seems particularly relevant for the modelling of *CDKL5*-related disease. In fact, glutamatergic excitatory neurotransmission has been reported to be altered in RTT due to *MECP2* mutations.¹³ Considering the interaction between *CDKL5* and *MeCP2* and their common involvement in RTT, it is conceivable that *CDKL5* absence might affect, at least in part, the same neuronal circuits. If this is the case, we could expect our cells to show a phenotype similar to that recently reported for *MECP2*-mutated hiPSCs-derived neurons.¹⁸ However, in mouse brain, *CDKL5* is expressed at high levels also in GABAergic neurons.²⁰ It will be thus interesting to differentiate our hiPSCs into both glutamatergic and GABAergic neurons in order to check whether a phenotype can be observed in both neuronal populations or whether *CDKL5* absence specifically affects one neuronal type.

In conclusion, we report here the generation of iPSCs from two patients with *CDKL5* mutations. We demonstrated that the female *CDKL5*-mutated iPSCs maintain X-chromosome inactivation, and we could identify clones expressing either the wild-type or the mutant *CDKL5* allele. Neuronal differentiation experiments indicate that the cells can be differentiated into neurons and are thus suitable to model disease pathogenesis. However, expression analyses on the mature cultures suggest that methods to selectively isolate neuronal precursors are necessary if we want to perform accurate quantitative comparisons between the cells derived from different clones. The identification of a clone from the female patient expressing exclusively the wild-type *CDKL5* allele represents a very exciting result, as this clone potentially represents the ideal isogenic control, genetically identical to those derived from the same patient but expressing the mutant allele, to study the effect of the mutation without 'perturbations' related to differences in genetic background.

CONFLICT OF INTEREST

The authors declare no conflict of interest.

ACKNOWLEDGEMENTS

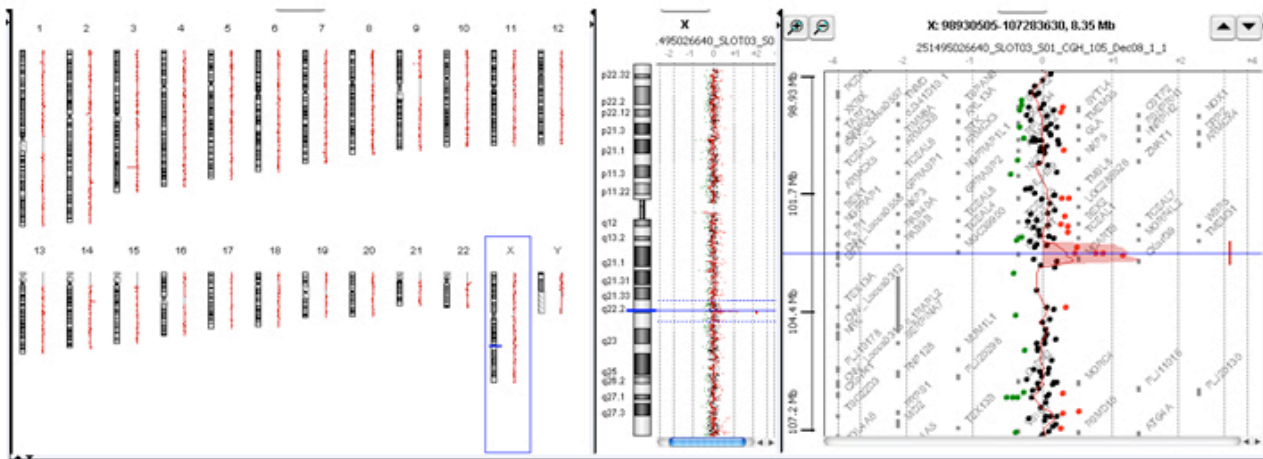
The authors are grateful to Peter Pasceri and Tadeo Thompson for technical assistance. We acknowledge 'Cell Lines and DNA Bank of Rett syndrome and X-linked mental retardation' (Medical Genetics-Siena) - Telethon Genetic

Biobank Network (Project No. GTB07001C to AR), a Canadian Institutes of Health Research grant (MOP-102649 to JE), a Natural Sciences and Engineering Research Council of Canada Postgraduate Scholarship Doctoral Award (to AYLC), Telethon grant GGP09117 and a grant by A.I.R. (Associazione Italiana Rett) (to AR).

- 1 Chahrouh M, Zoghbi HY: The story of Rett syndrome: from clinic to neurobiology. *Neuron* 2007; **56**: 422–437.
- 2 Hagberg BA, Skjeldal OH: Rett variants: a suggested model for inclusion criteria. *Pediatr Neurol* 1994; **11**: 5–11.
- 3 Rolando S: Rett syndrome: report of eight cases. *Brain Dev* 1985; **7**: 290–296.
- 4 Hanefeld F: The clinical pattern of the Rett syndrome. *Brain Dev* 1985; **7**: 320–325.
- 5 Zappella M: The preserved speech variant of the Rett complex: a report of 8 cases. *Eur Child Adolesc Psychiatry* 1997; **6**: 23–25.
- 6 Scala E, Ariani F, Mari F et al: CDKL5/STK9 is mutated in Rett syndrome variant with infantile spasms. *J Med Genet* 2005; **42**: 103–107.
- 7 Ariani F, Hayek G, Rondinella D et al: FOXG1 is responsible for the congenital variant of Rett syndrome. *Am J Hum Genet* 2008; **83**: 89–93.
- 8 Matijevic T, Knezevic J, Slavica M, Pavelic J: Rett syndrome: from the gene to the disease. *Eur Neurol* 2009; **61**: 3–10.
- 9 Chahrouh M, Jung SY, Shaw C et al: MeCP2, a key contributor to neurological disease, activates and represses transcription. *Science* 2008; **320**: 1224–1229.
- 10 Guy J, Hendrich B, Holmes M, Martin JE, Bird A: A mouse *Mecp2*-null mutation causes neurological symptoms that mimic Rett syndrome. *Nat Genet* 2001; **27**: 322–326.
- 11 Chen RZ, Akbarian S, Tudor M, Jaenisch R: Deficiency of methyl-CpG binding protein-2 in CNS neurons results in a Rett-like phenotype in mice. *Nat Genet* 2001; **27**: 327–331.
- 12 Shahbazian M, Young J, Yuva-Paylor L et al: Mice with truncated MeCP2 recapitulate many Rett syndrome features and display hyperacetylation of histone H3. *Neuron* 2002; **35**: 234–254.
- 13 Chao HT, Zoghbi HY, Rosenmund C: MeCP2 controls excitatory synaptic strength by regulating glutamatergic synapse number. *Neuron* 2007; **56**: 58–65.
- 14 Takahashi K, Tanabe K, Ohnuki M et al: Induction of pluripotent stem cells from adult human fibroblasts by defined factors. *Cell* 2007; **131**: 861–872.
- 15 Marchetto MC, Winner B, Gage FH: Pluripotent stem cells in neurodegenerative and neurodevelopmental diseases. *Hum Mol Genet* 2010; **19**: R71–R76.
- 16 Chamberlain SJ, Chen PF, Ng KY et al: Induced pluripotent stem cell models of the genomic imprinting disorders Angelman and Prader-Willi syndromes. *Proc Natl Acad Sci USA* 2010; **107**: 17668–17673.
- 17 Urbach A, Bar-Nur O, Daley GQ, Benvenisty N: Differential modeling of fragile X syndrome by human embryonic stem cells and induced pluripotent stem cells. *Cell Stem Cell* 2010; **6**: 407–411.
- 18 Marchetto MC, Carromeu C, Acab A et al: A model for neural development and treatment of Rett syndrome using human induced pluripotent stem cells. *Cell* 2010; **143**: 527–539.
- 19 Mari F, Azimonti S, Bertani I et al: CDKL5 belongs to the same molecular pathway of MeCP2 and it is responsible for the early-onset seizure variant of Rett syndrome. *Hum Mol Genet* 2005; **14**: 1935–1946.
- 20 Rusconi L, Salvatoni L, Giudici L et al: CDKL5 expression is modulated during neuronal development and its subcellular distribution is tightly regulated by the C-terminal tail. *J Biol Chem* 2008; **283**: 30101–30111.
- 21 Bertani I, Rusconi L, Bolognese F et al: Functional consequences of mutations in CDKL5, an X-linked gene involved in infantile spasms and mental retardation. *J Biol Chem* 2006; **281**: 32048–32056.
- 22 Carouge D, Host L, Aunis D, Zwiler J, Anglard P: CDKL5 is a brain MeCP2 target gene regulated by DNA methylation. *Neurobiol Dis* 2010; **38**: 414–424.
- 23 Kameshita I, Sekiguchi M, Hamasaki D et al: Cyclin-dependent kinase-like 5 binds and phosphorylates DNA methyltransferase 1. *Biochem Biophys Res Commun* 2008; **377**: 1162–1167.
- 24 Chen Q, Zhu YC, Yu J et al: CDKL5, a protein associated with Rett syndrome, regulates neuronal morphogenesis via Rac1 signaling. *J Neurosci* 2010; **30**: 12777–12786.
- 25 Dracopoli N, Haines J, Korf B, Morton C, Seidman C, Smith D: *Current Protocols in Human Genetics*. NY: John Wiley & Son, Inc., 2000.
- 26 Hotta A, Cheung AY, Farra N, et al: Isolation of human iPS cells using EOS lentiviral vectors to select for pluripotency. *Nat Methods* 2009; **6**: 370–376.
- 27 Allen RC, Zoghbi HY, Moseley AB, Rosenblatt HM, Belmont JW: Methylation of HpaII and HhaI sites near the polymorphic CAG repeat in the human androgen-receptor gene correlates with X chromosome inactivation. *Am J Hum Genet* 1992; **51**: 1229–1239.
- 28 Pankratz MT, Li XJ, Lavaute TM, Lyons EA, Chen X, Zhang SC: Directed neural differentiation of human embryonic stem cells via an obligated primitive anterior stage. *Stem Cells* 2007; **25**: 1511–1520.
- 29 Li XJ, Zhang X, Johnson MA, Wang ZB, Lavaute T, Zhang SC: Coordination of sonic hedgehog and Wnt signaling determines ventral and dorsal telencephalic neuron types from human embryonic stem cells. *Development* 2009; **136**: 4055–4063.
- 30 Meloni I, Parri V, De Filippis R et al: The XLMR gene *ACSL4* plays a role in dendritic spine architecture. *Neuroscience* 2009; **159**: 657–669.
- 31 Artuso R: Early-onset seizure variant of Rett syndrome: definition of the clinical diagnostic criteria. *Brain Dev* 2010; **32**: 17–24.
- 32 Elia M, Falco M, Ferri R et al: CDKL5 mutations in boys with severe encephalopathy and early-onset intractable epilepsy. *Neurology* 2008; **71**: 997–999.
- 33 Laurent C: Dynamic changes in the copy number of pluripotency and cell proliferation genes in human ESCs and iPSCs during reprogramming and time in culture. *Cell Stem Cell* 2011; **8**: 106–118.
- 34 Hussein M: Copy number variation and selection during reprogramming to pluripotency. *Nature* 2011; **471**: 58–62.
- 35 Goto T, Monk M: Regulation of X-chromosome inactivation in development in mice and humans. *Microbiol Mol Biol Rev* 1998; **62**: 362–378.
- 36 Nichols J, Smith A: Naive and primed pluripotent states. *Cell Stem Cell* 2009; **4**: 487–492.
- 37 Maherali N, Sridharan R, Xie W et al: Directly reprogrammed fibroblasts show global epigenetic remodeling and widespread tissue contribution. *Cell Stem Cell* 2007; **1**: 55–70.
- 38 Hall LL, Byron M, Butler J et al: X-inactivation reveals epigenetic anomalies in most hESC but identifies sublines that initiate as expected. *J Cell Physiol* 2008; **216**: 445–452.
- 39 Tchieu J, Kuoy E, Chin MH et al: Female human iPSCs retain an inactive X chromosome. *Cell Stem Cell* 2010; **7**: 329–342.
- 40 Cheung AY: Isolation of MECP2-null Rett Syndrome patient hiPS cells and isogenic controls through X-chromosome inactivation. *Hum Mol Genet* 2011; **20**: 2103–2115.
- 41 Zhang SC, Wernig M, Duncan ID, Brustle O, Thomson JA: *In vitro* differentiation of transplantable neural precursors from human embryonic stem cells. *Nat Biotechnol* 2001; **19**: 1129–1133.
- 42 Hu BY, Weick JP, Yu J et al: Neural differentiation of human induced pluripotent stem cells follows developmental principles but with variable potency. *Proc Natl Acad Sci USA* 2010; **107**: 4335–4340.
- 43 Yuan S: Cell-surface marker signatures for the isolation of neural stem cells, glia and neurons derived from human pluripotent stem cells. *PLoS ONE* 2011; **6**: e17540.
- 44 Carson CT, Aigner S, Gage FH: Stem cells: the good, bad and barely in control. *Nat Med* 2006; **12**: 1237–1238.

Supplementary Information accompanies the paper on European Journal of Human Genetics website (<http://www.nature.com/ejhg>)

A



B

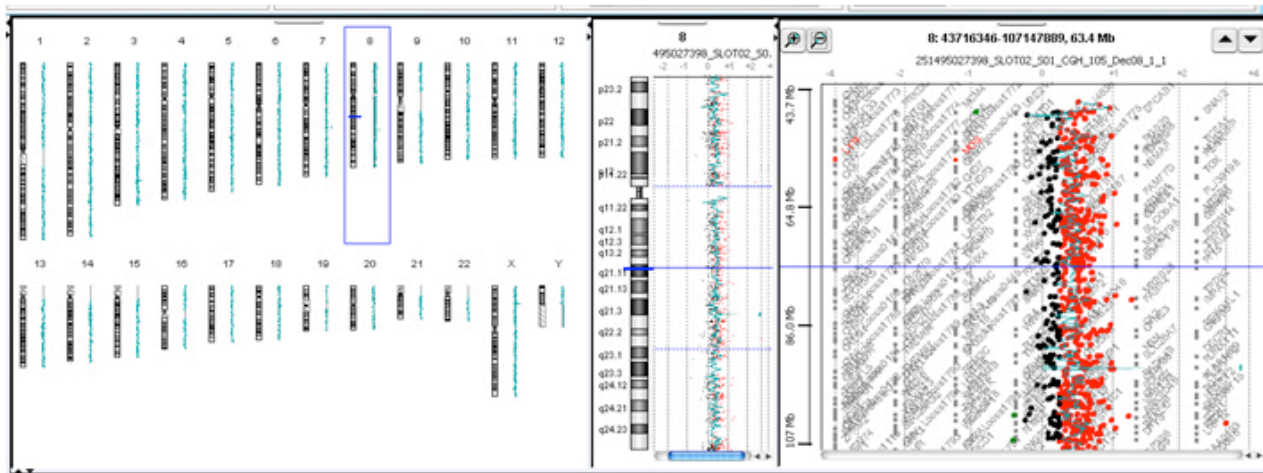


Figure S1

Figure S1: Array-CGH analysis. CNVs identified by array-CGH analysis in iPS cells are presented. An overview of array results for all chromosomes is shown on the left. On the right, there is an higher magnification of the identified CNVs. Each dot represents a single probe (oligo) spotted on the array. Oligos with equal fluorescence intensity ratio between sample and reference have a value of zero. Copy number gains shift the ratio to the right (value of about +1, red dots). **A.** A representative image of the duplication in Xq22.2 that was identified in parental fibroblasts and in the three clones from patient 1. **B.** A trisomy of chromosome 8 is present in clone #52 derived from patient 2.

Table S1: primers for neuronal markers

Gene	Forward primer	Reverse primer	Melting temperature
VGLUT1	GTCTGGGCTTCTGCATCAG	CTGGAATCTGAGTGACAATG	60°C
VGLUT2	ACATCCATGCCAGTCTATGC	CTTTCTCACTGTCGTAGTTG	60°C
TBR1	TGCATGTGGTGGAAGTGAAC	GTCACAGCCGGTGTAGATC	52°C
GAD67	TTGACTGCAGAGACACCTTG	ACCATCCAACCTTCTCTCTC	60°C
GFAP	GATTGAGTCGCTGGAGGAG	TGGAGCGGTACCACTCTTC	60°C

Result 3.2

**Set up of a protocol for the analysis of morphological alterations in CDKL5
neurons**

3.2: Set up of a protocol for the analysis of morphological alterations in CDKL5 neurons

Although CDKL5 role in neurons is far from being clarified, recently it has been demonstrated that in rat brain it is essential for neuronal morphogenesis, providing the first evidence of a cellular mechanism that may be responsible for the developmental effects caused by *CDKL5* mutations and for the observed disease phenotype¹⁵. However so far it is not clear whether the alterations identified in rat neurons correspond to the situation in affected human neurons. Interestingly, in patients with neurodevelopmental disorders such as nonsyndromic mental retardation and RTT an abnormal morphology is a characteristic feature of neurons^{81,83}. Neuropathology studies on *Mecp2*-deficient mice have reported that mutant brains exhibit a substantial reduction in both weight and neuronal cell size⁵⁹. The same results are observed throughout the cortical and subcortical region of post-mortem RTT human brains⁸⁴. Moreover, recent data on MECP2-iPSCs derived neurons have documented a consistent reduction in cell soma size of neurons carrying different MeCP2 mutations when compared to normal controls⁶³. To better understand whether CDKL5-iPSCs derived human neurons exhibited any consistent morphological alteration when compared to normal controls we decided to set up a protocol based on the use of lentiviruses expressing EGFP in order to visualize neuronal anatomy. Considering that neural differentiation results in variable and heterogeneous cultures of neurons, glia and undifferentiated cells, we decided to test two different lentiviruses: one driving ubiquitous EGFP expression, and one driving neurospecific GFP expression under the control of synapsin promoter. Furthermore, in order to assess whether the soma size reduction observed for MECP2-iPSCs derived neurons is present also in CDKL5-iPSCs derived neurons, we performed a cell soma size analysis comparing mutated neurons with normal controls.

3.2.1 Materials and Methods

Cell culture. HEK293T and PC12 cells were maintained in DMEM High glucose (Invitrogen) supplemented with 10% (vol/vol) FBS, 10 mM non-essential amino acids, 50 U/ml penicillin, 50 mg/ml streptomycin. Neuronal differentiation of iPSCs was performed according to a protocol established for human ESC^{73,85} and results 1. (Fig. 1)

Lentiviral vectors preparation. PLL3.7 plasmid for ubiquitous GFP expression was obtained from Dr Vania Broccoli (San Raffaele, Milan). Syn-EGFP plasmid, containing EGFP under the control of Synapsin-1 promoter, was obtained from Addgene (ID 19975). Plasmid identity was confirmed by enzymatic digestion and direct sequencing. To produce lentiviral vectors we transfected each plasmid into HEK293T cells together with four packaging plasmids encoding the lentiviral *Gag-pol*, *Tat*, *Rev* and *VSV-G* genes, also obtained from Addgene (ID 12251, 22502, 12253, 8454). Plasmids were co-transfected into HEK293T cells using Lipofectamine 2000 reagent (Invitrogen) according to the manufacturer's instructions. Two days after plasmid transfection, virus stocks were harvested, filter sterilized and used for virus titration. Virus titer was determined by checking the percentage of EGFP positive cells in PC12 and HEK293T cells. One day before titration cells were seeded at a density of 10^5 cells per well of a 12-well plate containing collagen-coated coverslips. The day after the medium was changed with pre-warmed medium containing polybrene to a final concentration of 8 $\mu\text{g/ml}$ and several virus dilutions were added. Two days after infection cells were fixed with PFA 4% and immunostained for GFP (AbCam). DAPI was used to stain cell nuclei. At least 15 fields for each virus dilution were acquired under the fluorescent microscope and the total number of cells (DAPI nuclear staining) and the number of GFP⁺ cells was determined. The viral titer (IU = infective units) was calculated with the following formula: Viral titer (IU/ml)=[Infected cell number in a well] \times [EGFP⁺% / 100]/[Amount of virus used (ml)].

Lentiviral infection of neurons. To test the two lentiviruses we used a normal male control iPS clone derived from a male BJ fibroblast line (Cell line n° CRL-2522) from ATCC (see Results 1). Neuronal cultures were infected with several amounts of virus and at different days during the differentiation course. Considering that the neuronal differentiation process lasts 70 days and that the percentage of neurons in cultures is variable we decided to not proceed with trypsinization of neuronal cultures and cell count. The amount of virus to use was decided on

the basis of the viral titer obtained for PC12 and HEK293T cells. Polybrene at 8 µg/ml was added to neuronal medium for the infection. About 16 hours after infection the medium was changed with fresh one. After infection, medium was changed every two days till Day 70.

Immunostaining. To confirm the identity of the obtained neurons immunofluorescence was performed with standard protocols (see Results 1) using the generic neuronal marker MAP2 (AbCam). An anti-GFP antibody (AbCam) was used to enhance GFP fluorescence while DAPI was used to stain cell nuclei (Sigma Aldrich). Cells were visualized with an Axioscop 40FL (Zeiss) microscope connected to a computer.

Morphometric analysis. To analyse soma size of neurons we acquired pictures at high magnification (100X). Images were analysed using ImageJ software. At least 15 cells for each clone were analysed. In order to avoid bias due to the difficulty to accurately delineate the cell soma, we decided to measure nuclear size. For each neuron, nuclear boundaries were delineated using ImageJ and the program measured the area expressed in arbitrary unit. An iPSC clone bearing the *MECP2* mutation p.R306C obtained from Dr James Ellis (Sick Children Hospital, Toronto) was used as internal control to evaluate the accuracy of the method.

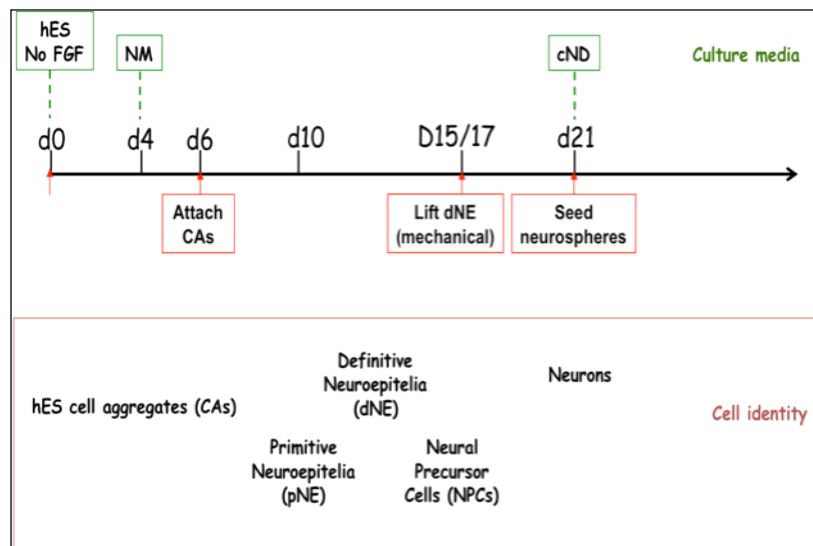


Fig. 1. Neuronal differentiation Protocol. The scheme summarizes the neuronal differentiation protocol applied to induce iPSC toward neuronal fate.

3.2.2 RESULTS

Lentiviruses testing

Neuronal differentiation results in variable and heterogeneous cultures of neurons, glia and undifferentiated cells. In order to obtain isolated neuronal cells suitable for morphological analysis we thus decided to test two different lentiviruses expressing EGFP: one driving ubiquitous GFP expression and one expressing GFP only in neurons, respectively PLL3.7 and Syn-EGFP. The titer of the lentiviral preparations was calculated in PC12 and HEK293T cells and was 3×10^4 IU/ml for Syn-EGFP and $4,9 \times 10^5$ IU/ml for PLL3.7. Concerning Syn-EGFP, HEK293T cells did not display GFP expression, confirming its neurospecificity.

PLL3.7

Neuronal cultures plated on Coverslips (CVS) were initially infected at Day 66 of neuronal differentiation with 100 μ l of PLL3.7 (3×10^3 IU). At Day 70 cells were fixed and immunostained for GFP and MAP2. A first observation indicated that mature cultures contained mostly non-neuronal GFP+ cells; however, it was possible to distinguish some isolated neurons and some structures resembling dendritic spines could be identified, although GFP intensity was too low (Fig. 2 A-D). Considering these initial results we decided to proceed with another infection, infecting the neuronal cultures 7 days before the end of the differentiation course (day 62), since we hypothesized that more time was necessary for neurons to express GFP at sufficient levels. We used the same amount of virus. Cells were fixed at day 70 and immunostained for GFP and MAP2. With this second attempt we confirmed the result obtained in the first experiment. Mature cultures contained both non-neuronal and neuronal cells positive for GFP, with a prevalence of the first, making it difficult to distinguish isolated neurons although in some isolated cells spines could be detected (FIG 3 A-B).

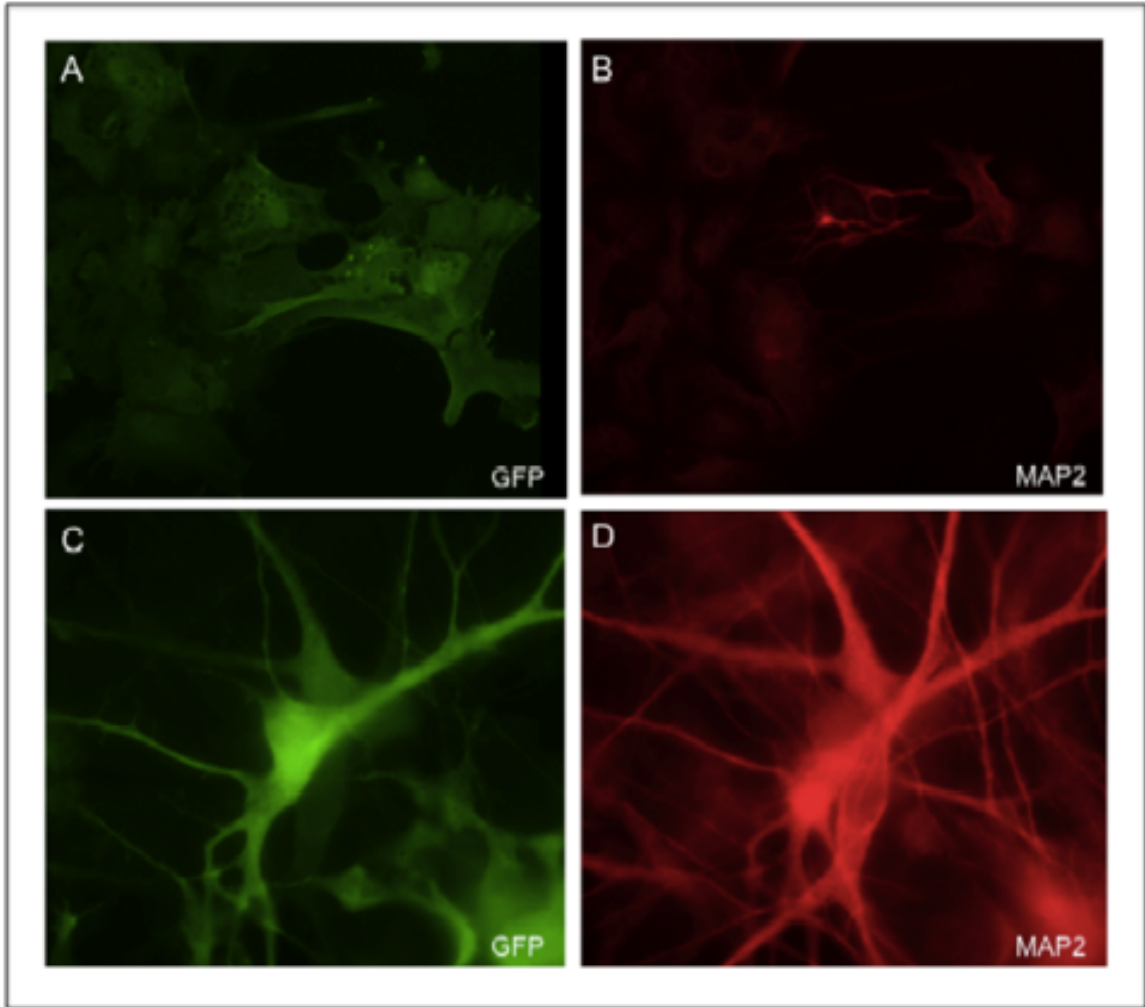


Fig. 2. PLL3.7 infection at Day 66. (A) Immunostaining with GFP reveals mostly non-neuronal GFP+ cells. (B) MAP2 staining of the same field shown in (A) to visualize neuronal cells. Comparing figure A and B we can observe that neuronal cells are not GFP+. Images are 20X magnification. (C) Higher magnification showing that GFP+ neurons can be identified but no dendritic spines can be visualized. (D) MAP2 staining confirming neuronal cells identity. Images are 20X magnification in A and B and 100X magnification in C and D.

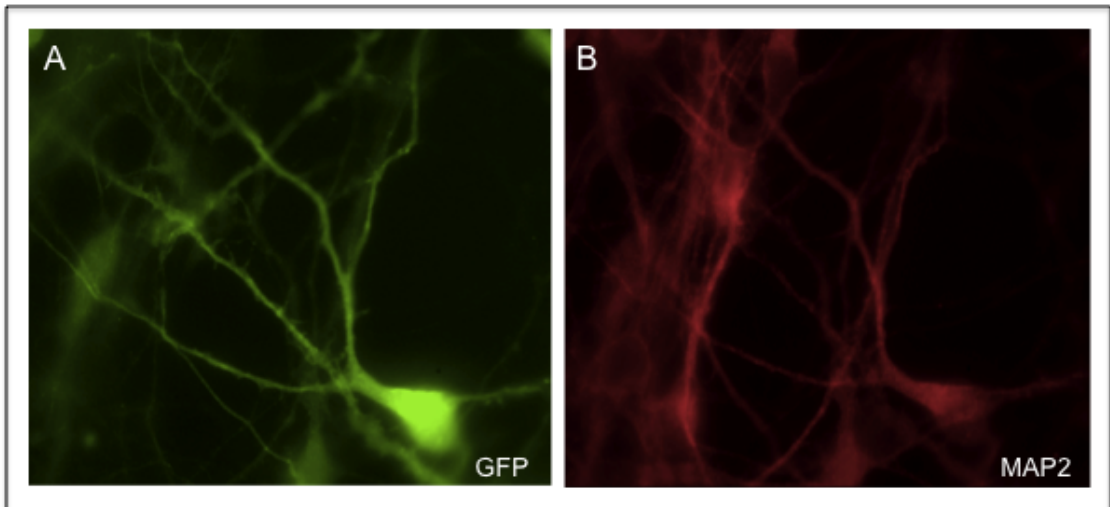


Fig. 3. PLL3.7- Day 62 infection. (A) GFP staining of an isolated neuron showing the presence of dendritic spines. **(B)** MAP2 staining to confirm neuronal identity.

SYN-EGFP

Neuronal cultures plated on CVS were initially infected at Day 66 of neuronal differentiation with 500 μl (1.5×10^4 IU) of SYN-EGFP. At Day 70 cells were fixed and immunostained for GFP and MAP2. At a first analysis we observed the presence of too many positive cells and it was difficult to discriminate single GFP+ neurons from the dense neuronal network arising in culture (Fig.4 A-B). In some cases it was however possible to visualize isolated neurons and to recognize some dendritic spines, but GFP intensity was too low to allow an accurate visualization of their morphology (Fig.4 C_D). Considering this initial examination we decided to proceed with another infection, infecting the neuronal cultures 7 days before the end of the differentiation course (day 62). However we decided to use a lower amount of SYN-EGFP virus: 250 μl and 100 μl , respectively. Cells were fixed at day 70 and immunostained for GFP and MAP2. Microscope analysis indicated that the lowest amount of virus was not a good choice to visualize GFP-positive neurons since very few positive cells could be seen in only one out of 3 infected CVS. On the contrary, 250 μl resulted to be a good amount to use in order to visualize isolated cells and identify the presence of spines, since GFP is well distributed along the neurites and spines could be clearly identified (Fig.5 A-B). However, we observed that there was a percentage of GFP+ neurons lacking visible spines, in accordance with recent literature data suggesting that some but not all neurons after the

differentiation process are completely mature Chamberlain⁹³. To finally evaluate whether increasing the time lapse between infection and observation could improve dendritic spines visualization without causing stress to neuronal cultures, we decided to proceed with two different infections respectively at 2 weeks and 1 week before the end of the neuronal differentiation course. We decided to use the same amount of virus, 250 μ l. Fluorescence microscope analysis of BJ neurons revealed that there was no significant difference between the two experiments and confirmed that 250 μ l is a good amount of SYN-EGFP lentivirus to use in further experiments for morphological analysis of neuronal cultures.

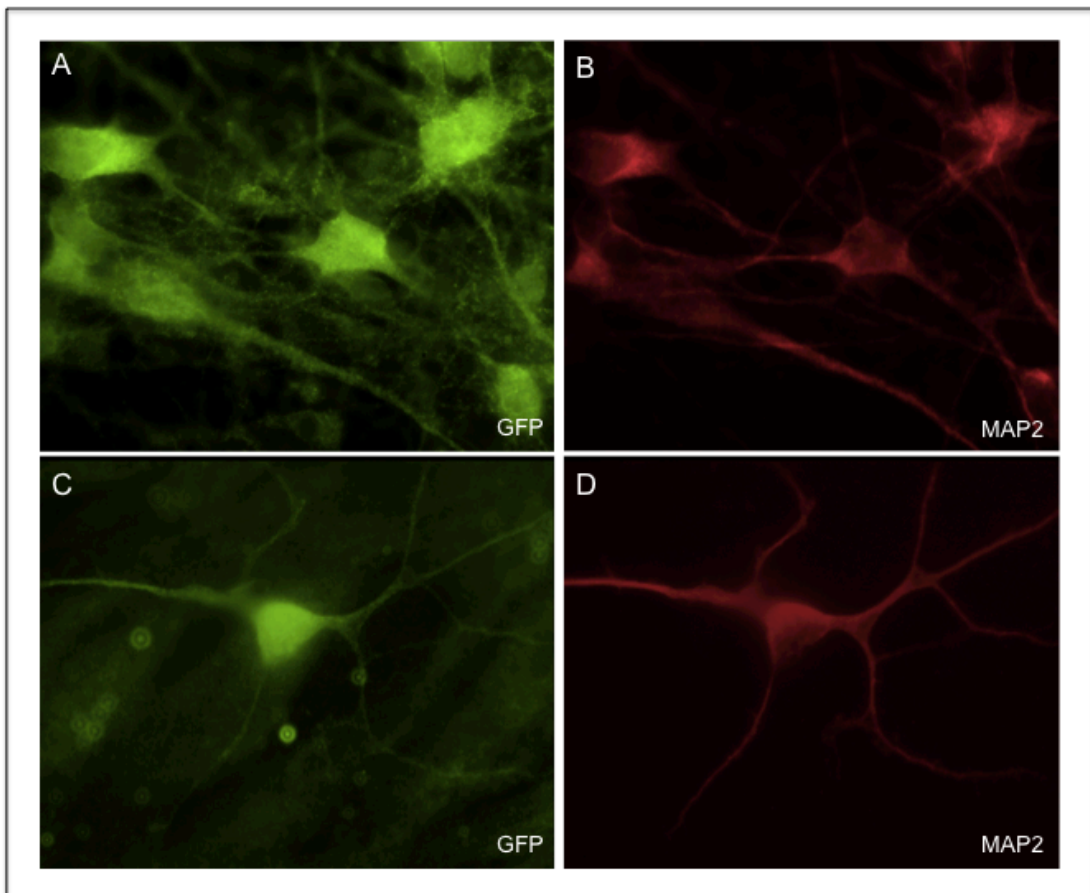


Fig. 4. SYN-EGFP- Day 66 infection with 500 μ l of virus. (A-B) GFP staining revealing the presence of several positive neuronal cells whose identity is confirmed by MAP2 staining. (C-D) Isolated neuronal cell with low GFP intensity hampering accurate visualization of its morphology. Images are 100X magnification.

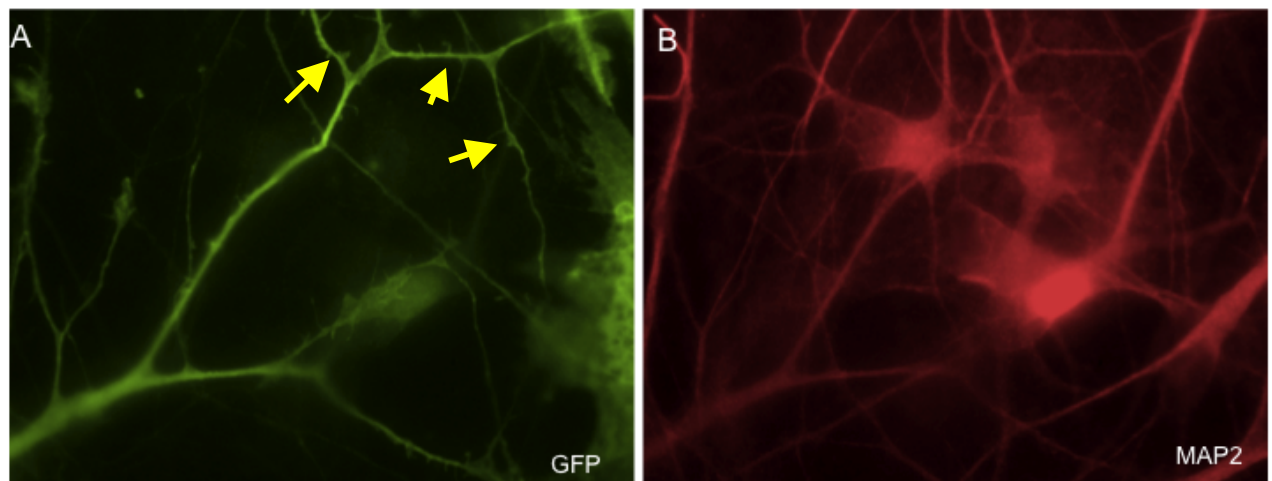


Fig. 5. SYN-EGFP Day 62 infection with 250 µl of virus. (A) GFP staining of an isolated neuron showing the presence of dendritic spines. (B) MAP2 staining confirming neuronal identity.

Soma size analysis

Neuropathology studies on RTT brains and histological results in *Mecp2*-deficient mice have demonstrated that neurons of RTT patients and mice are abnormal with a significant reduction in soma size^{59,84}. The same results have been recently obtained by morphological analysis of MECP2-iPSCs derived neurons^{63,76}. To determine whether similar alterations were present in our *CDKL5* mutated neurons compared to normal controls we decided to perform a soma size analysis on our neurons. To this aim, we derived neuronal cultures from 3 different iPSC clones: the iPSC-BJ clone (see above and Results 1 for details), used as normal control; an iPSC clone bearing the p-R306C *MECP2* mutation, used as internal positive control of the experiment; and the clone iPSC#58, obtained from the male patient reported in Results 1 (Patient2). Mature cultures were fixed at day 70 of neuronal differentiation and immunostained with MAP2 to identify neurons. Soma size measurement is not easy to perform accurately since it is arduous to define soma boundaries; for this reason we decided to measure nuclear size as visualized by DAPI staining. Using ImageJ software we calculated the nuclear area and perimeter of at least 15 cells for each clone (Fig.6 A-C). We observed that the neurons derived from the *MECP2*-mutated iPSC clone exhibited a significant reduction in nuclear size when compared to the neurons from the BJ control (13% reduction) (Fig.6 C). This result is consistent with previous findings in *Mecp2*^{-/-} mice and postmortem brain tissues from RTT patients^{59,84} and also with the data already reported for

MECP2-iPSCs derived neurons^{63,76}. However, as concerns our *CDKL5* patient (Patient 2) no significant difference in nuclear size was observed between BJ neurons and iPSC#58 derived neurons.

These results suggest that the use of the nuclear size for soma size calculation is reliable and gives consistent results. Experiments are ongoing to extend the sample size including three additional iPSC clones (#19, #46 and #20) derived from the female *CDKL5*-mutated patient (see Results 1) in order to confirm the initial results.

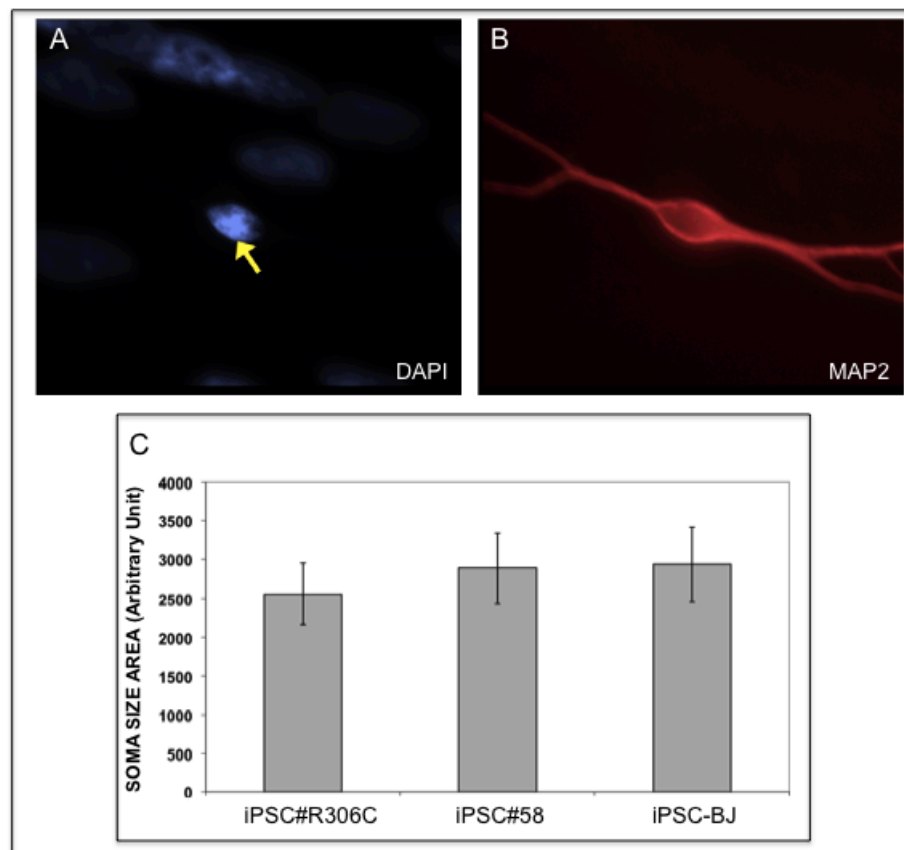


Fig. 6. Nuclear size evaluation of iPSC-derived neurons. A) Cell nuclei stained with DAPI. The nucleus indicated by the arrow belongs to a neuronal cell and has been used for soma size analysis. B) Neuronal cell stained with MAP2 used for nuclear size calculation. C) Nuclear size comparison between neurons derived from control iPSCs (iPSC-BJ), *MECP2*-mutated iPSCs (iPSC#R306C) and *CDKL5*-mutated iPSCs (iPSC#58). Bar graph shows the mean nuclear size area of iPSC-derived neurons. iPSC#R306C-derived neurons exhibit a reduction in nuclear size of about 13% compared with iPSC-BJ-derived neurons. iPSC#58-derived neurons do not show any difference in nuclear size respect to the normal control. Nuclear size area is expressed in an arbitrary unit as calculated by ImageJ program. MAP2 antibody was used to identify neurons.

Result 3.3

Gene expression profiling of iPSCs from *CDKL5* patients

3.3: Gene expression profiling of iPSCs from *CDKL5* patients

Brain is the primarily affected tissue in RTT patients. However expression studies in this tissue are difficult to carry out for obvious ethical reasons. Some studies have tried to overcome this limitation employing post-mortem tissues. However, this tissue may originate from late stages of the disorder and it might thus not be suitable to investigate the initial pathological processes of the disease ⁷⁹. Importantly, brain is characterized by cellular heterogeneity that might contribute to mask subtle expression differences. So far several gene expression studies involving *MECP2*-null samples have been performed on different tissues from RTT individuals and mouse models with *Mecp2* loss of function mutations ^{86,87}. However, the lists of mis-regulated genes derived from these studies are not-overlapping, probably due to the different approaches adopted, based on the use of clonal lymphoblastoid cell lines to avoid mosaicism, fibroblast strains from patients or post-mortem RTT brains ⁸⁸⁻⁹⁰. As concerns mouse models contrasting results may be due to the use of different RTT mouse models and also to the analysis of distinct brain regions such as cerebellum, cortex or midbrain ^{86,91}.

As concerns *CDKL5*, despite intensive research efforts, its function inside the neuron and the underlying molecular mechanisms remain still uncharacterized. *CDKL5* is a serine-threonine kinase. Kinase proteins are involved in the regulation of the activity of a huge range of different proteins, including many proteins that play essential roles in signalling cascades resulting in activation/repression of gene transcription. *CDKL5* protein seems to work in a molecular pathway common to that of *MeCP2*, a transcriptional regulator. In fact mutations in *CDKL5* are associated with some severe neurological symptoms that are occasionally reported in typical *MeCP2* cases such as infantile spasms, early onset epilepsy and hypsarrhythmia. Recent findings regarding a possible role of *CDKL5* in nuclear speckles organization, reinforce the hypothesis of an involvement of *CDKL5* in the regulation of gene expression ¹⁴. However expression profiling studies are hindered by the absence of a *CDKL5*-null mouse model, together with the absence of a good in vitro human cellular model. Very recently a first attempt of gene expression profiling has been performed on clonal primary cultures of fibroblasts derived from *CDKL5*-mutated patients leading to the identification of a total of 16 up-regulated and 20 down-regulated genes. Among these genes only *MAP3K5*, an apoptosis signal regulated kinase, was found to be down-regulated also in neuroblastoma-

derived SH-SY5Y cells transfected with an shRNA targeting *CDKL5*. MAP3K5 is involved in MAP kinase pathway that mediates signals leading to both differentiation and survival in neuronal cells. According to the authors its significant underexpression in human *CDKL5*-deficient cells may suggest that neurite outgrowth and synaptic plasticity may be altered in *CDKL5* mutated brains⁹². These data are in agreement with those obtained by Chen and colleagues, indicating that *CDKL5* acts as a critical regulator of neuronal morphogenesis through a signalling pathway involving the Rac1 GTPase¹⁵.

CDKL5, as *MECP2*, is located on the X chromosomes and undergoes X chromosome inactivation, so that female patients result in mosaic expression of mutant or wild type *CDKL5* in each of their cells; analysis of gene expression profile in girls will be thus compromised by unpredictable patterns of XCI. However we recently have confirmed previous data on X inactivation in iPSCs, indicating that human iPSCs can retain an inactive X-chromosome in a clonal pattern, with one of the two X chromosomes exclusively inactivated in all the cells of a single clone^{63,75,76}. Indeed we have obtained clones derived from the same patient but expressing either the wild type or the mutated *CDKL5* allele (Result 1), thus overcoming the functional mosaicism resulting from XCI. In addition these cells are genetically identical and differ only for *CDKL5* expression and they thus represent the ideal tool to analyse the consequences of *CDKL5* absence without confounding effects due to different genetic background.

On the basis of all these considerations we decided to perform gene expression analysis on iPSC clones derived from *CDKL5* mutated patients, in order to detect candidate genes that might be involved in neurogenetic processes and thus contribute to gain new insights into the mechanisms underlying *CDKL5* function in neuronal development. To this aim, we compared the global gene expression pattern at the transcript level in matched pairs of wild-type and mutant iPSCs clones from two different patients.

3.3.1 Experimental procedures

iPSC clones. iPSCs clones were derived from fibroblasts of two different *CDKL5*-mutated patients (Result 1): a female patient (Patient 1) with the early-onset seizures variant of RTT and an early truncating mutation (p.Q347X) and a male patient (Patient 2) with severe encephalopathy and early-onset intractable epilepsy that carries a missense mutation

(p.T288I) affecting the catalytic kinase domain. For patient 1 we selected 2 different iPSC clones, one expressing the wt allele, thus used as normal control (iPSC#20), and the other expressing the mutated *CDKL5* allele (iPSCs#46) (See Results 1). For patient 1 we selected only one fully characterized clone (iPSCs#58) and used a normal male iPSC clone derived from a male BJ fibroblast line from ATCC as control (iPSC-BJ). Clones were maintained in mTeSR1 supplied with puromycin using standard procedures.

RNA isolation. Total RNA was extracted from iPSC clones with the Qiagen RNeasy kit (Qiagen) according to manufacturer recommended protocol. Prior to array hybridization RNA quality and quantity were assessed with the RNA 6000 Nano Assay using 2100 Bioanalyzer (Agilent Technologies). For clones derived from the female patient, the exclusive expression of only one *CDKL5* allele was confirmed by RT-PCR and sequencing.

cDNA labelling and microarray hybridization. Agilent Whole Human Genome 4X44K microarrays and Two-Color Microarray-Based gene expression Analysis (Quick Amp Labeling) Protocol were used for global gene expression analysis. 500 ng of total RNA from control and mutated samples was used to prepare amplified and labeled cRNA using Quick-Amp Labeling Kit (Agilent). Control and mutated samples were labelled with Cy3-dCTP and Cy5-dCTP respectively. For each clone, four technical replicates were performed to control technical bias. Following purification with Qiagen RNeasy kit (Qiagen), according to protocol instructions, cRNA was quantified using NanoDrop ND-1000 UV-VIS Spectrophotometer in order to determine the yield and specific activity of each reaction. For each replicate 825 ng of labeled control cRNA was combined with 825 ng of labelled mutated cRNA. The combined reactions were then applied to cRNA microarray. Hybridization was carried out at 65°C for 17 hr in a hybridization oven. Blocking agent was added according to the protocol.

Microarray data analysis. Following hybridization, microarrays were washed and scanned with an Agilent DNA microarray scanner (G2505B) and analysed by Agilent Feature Extraction Software v9.5. The resulting text files were imported into Gene Spring GX software v11.5 for processing and analysis of microarray data. Significantly modulated genes were defined as those with absolute fold change (FC) > 1.5. To translate the data in a more meaningful biological context and to identify candidate genes, functional analysis of the selected genes has been performed using available on-line databases (<http://www.genecards.org/>; <http://genome.ucsc.edu/>; <http://www.uniprot.org/>) in order to

identify differentially expressed genes that might be involved in neurogenetic processes, thus playing a possible role in the pathophysiology of CDKL5-related disorders.

3.3.2 Results

Microarray analysis of matched iPSC clones

In order to identify genes specifically regulated by CDKL5, we carried out an expression profile experiment on iPSC clones derived from two different *CDKL5*-mutated patients. For the female patient we selected as normal control the iPSC#20 that expresses only the wt allele due to skewed X chromosome inactivation, while for the male patient we used the BJ clone (see also Results 1). For each patient we performed direct competitive hybridization between WT and mutated clones; hybridization of labelled RNA on Agilent Whole Human Genome 4X44K microarrays was carried out in four technical replicates, providing a total of eight chip hybridizations on two microarray slides. The expression signals were extracted from arrays using Agilent Feature Extraction Software v9.5. The software automatically finds and places microarray grids, accurately determines feature intensities and ratios, flags outlier pixels and calculates statistical confidence (www.genomics.agilent.com). At the end of this analysis the software generates a QC report and the data files that can be used for further analysis. The QC report (GE 2-color with Agilent spike-ins) allows the evaluation of the correct grid placement and of microarray scan quality and reliability. For further processing and interpretation, we imported the data files into Gene Spring GX software v11.5. Fig. 1A summarizes the analysis procedure applied to our data. For each patient, technical replicates were grouped together. We decided to calculate differences in gene expression level between WT and mutant clones for each patient separately (matched pairs). Before starting the analysis, data were qualitatively assessed using defined flag import settings, in order to remove those entities that are not reliably detected, and pre-processed with the “baseline transformation to median of all samples” step. As a first approach to gene expression profiling, we selected genes on the basis of their fold change (FC). Significantly altered genes were defined as those with absolute FC > 1.5. The analysis returned a list of 295 dysregulated genes for patient 2 (Entity list 1) and 276 genes for Patient 1 (Entity list 2). Since our aim was to identify genes that might be involved in a common regulatory circuit with CDKL5 and thus be influenced by its deficiency we then compared the gene lists obtained for each patient using the Venn diagram approach in order to verify the presence of

overlapping genes (Fig 1B). This comparison revealed 11 differentially expressed genes in common between the two patients; two of these genes were altered in opposite directions in the two samples (up-regulated in one patient and down-regulated in the other) and were thus excluded from further analyses (Table 1). We inspected our list on the basis of gene function and expression patterns in order to identify potentially relevant genes. One down-regulated gene *GRIP1* (glutamate receptor interacting protein 1) seems particularly interesting since it is present in both glutamatergic and GABAergic synapses and seems to play a role in postsynaptic localization of AMPA receptors that are involved in synaptic plasticity (Song I et al., 2002; Santos SD et al., 2009).

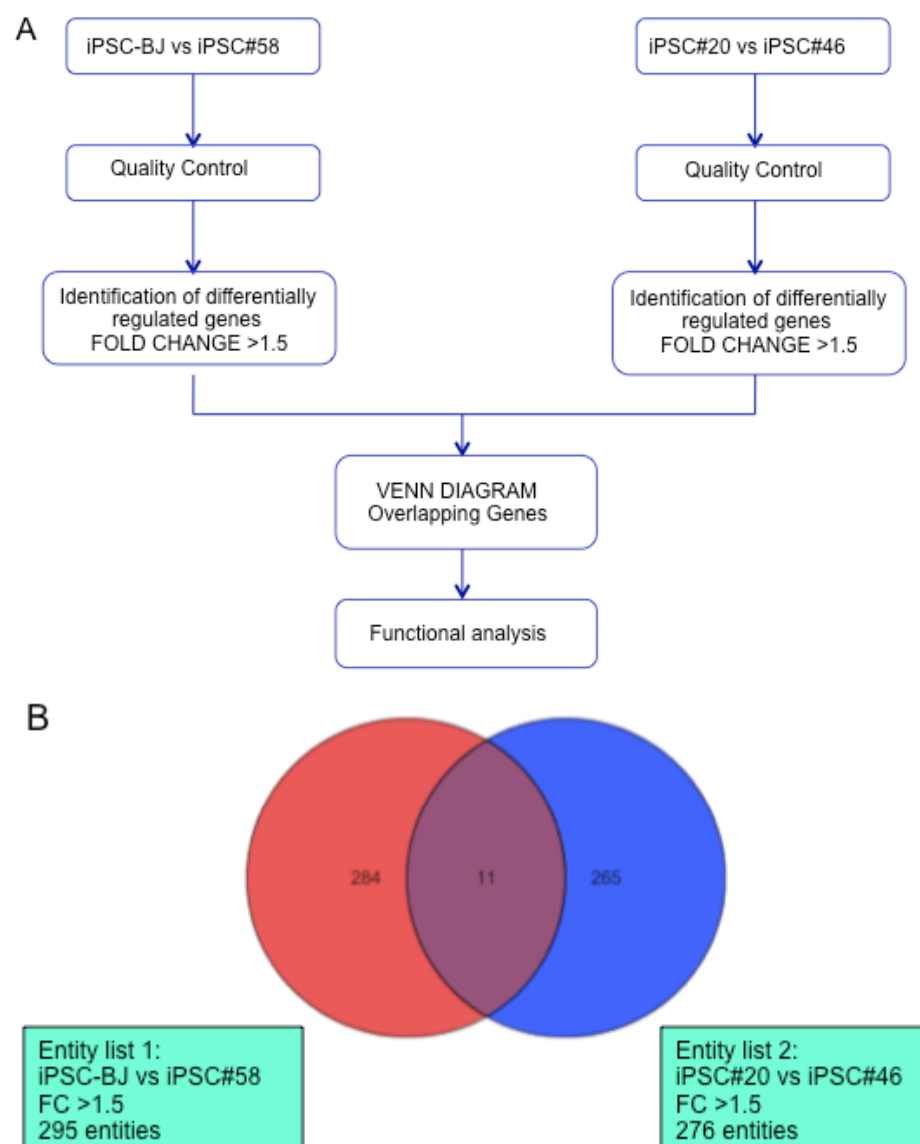


Fig. 1. (A) Flow chart summarizing the analysis procedure. (B) Venn Diagram obtained by overlapping the single entity lists for each “WT vs mutated” couple of samples. A total of 11 genes are in common between the two couples.

Gene symbol	Gene Name	Regulation	Fold change	Function
<i>GRID1</i>	glutamate receptor, ionotropic, delta 1	down	- 1.9	This gene encodes a subunit of glutamate receptor channels. These channels mediate most of the fast excitatory synaptic transmission in the central nervous system and play key roles in synaptic plasticity.
<i>SLC38A10</i>	solute carrier family 38, member 10	down	- 1.7	Putative sodium-dependent amino acid/proton antiporter
<i>SLC23A3</i>	solute carrier family 23 (nucleobase transporters), member 3	up	+ 2.5	unknown
<i>LST1</i>	leukocyte specific transcript 1	up	+ 2.5	Possible role in modulating immune responses. Induces morphological changes including production of filopodia and microspikes when overexpressed in a variety of cell types and may be involved in maturation of dendritic cells of the immune system. Isoform 1 and isoform 2 have an inhibitory effect on lymphocyte proliferation
<i>RESP18</i>	regulated endocrine-specific protein 18	up	+ 2.3	May play an important regulatory role in corticotrophs (By similarity). Found in alpha, beta and delta cells in the pancreatic islets.
<i>ODF4</i>	outer dense fiber of sperm tails 4	down	- 1.7	This gene encodes a protein that is localized in the outer dense fibers of the tails of mature sperm. This protein is thought to have some important role in the sperm tail.
<i>IGKV3D-20-001</i>	immunoglobulin kappa variable 3D-20	down	-1.9	Putative uncharacterized protein

Table 1. List of common differentially expressed genes between the two patients analysed.

4. DISCUSSION AND FUTURE PERSPECTIVES

4. Discussion and future perspectives

CDKL5 gene has been isolated in 1998 by Montini and colleagues while mapping Xp22 region ¹. The first mutations in this gene have been reported in two female patients with ISSX ². After that several groups have described mutations in *CDKL5* in patients with seizures appearing soon after birth and severe mental intellectual disabilities. Up to now the phenotypic spectrum of *CDKL5* abnormalities has become broader, including clinical features resembling those of other neurodevelopmental disorders. In particular, most of the cases have been diagnosed with early onset seizures variant of RTT and X-linked infantile spasm syndrome, with a prevalence of the former suggesting that this could be the predominant phenotype caused by *CDKL5* mutations. ^{17,20}. Since its molecular characterization has started only in 2005, the protein remains largely uncharacterized, mainly due to the absence of both a mouse model and a satisfactory in vitro human cellular model. Considering the recent advancements in the use of iPSCs technology to model neurological and neurodevelopmental disorders in vivo, we also decided to employ this technique to establish a human cellular model that can recapitulate *CDKL5*-related disorders with the aim to better clarify the role of *CDKL5* in human neurons. To this purpose we reprogrammed fibroblasts from 2 different patients, a male presenting with severe encephalopathy and early onset intractable epilepsy and a girl with the early onset seizures variant of RTT. iPSCs could be successfully derived from both patients and further induced toward neuronal fate. Although phenotypic characterization of these cells is still ongoing, our present results indicate that *CDKL5* absence does not impair the capacity of iPSCs to differentiate toward a neuronal fate, thus suggesting. Moreover the mutated iPSC clones and the WT ones have similar efficiency of differentiation toward neuronal lineage, thus indicating that *CDKL5* is not essential in the preliminary phases of differentiation. A more accurate analysis of the neuronal differentiation course will be necessary to verify possible effects due to *CDKL5* absence in the following differentiation steps.

iPSCs have been used in the attempt to model neurodegenerative and neurodevelopmental disorders including X-linked disorders. Interestingly, several groups have demonstrated that human iPSCs retain an inactive X-chromosome in clonal pattern, with one of the two X chromosomes exclusively inactivated in all the cells of a single clone ^{75,76}. However some contrasting results have emerged as reported by Marchetto and colleagues indicating that X-inactivation is erased during reprogramming of iPSC and

restored only after neuronal differentiation⁶³. Considering that *CDKL5* is an X-linked gene and that XCI status in iPSCs is still controversial, we performed X-chromosome inactivation analysis on our iPSC clones. We observed that, upon reprogramming, our iPSC clones maintain XCI and interestingly each clone exclusively expresses the mutated or wild type allele, in agreement with similar observations by other groups^{75,76}. It is worth noting that we analysed the clones at different passage numbers and we could demonstrate that the same X chromosome remains active in each clone, irrespective of passage number, suggesting that XCI is consistently maintained upon cells expansion in culture and thus strengthening the hypothesis that XCI is not erased during reprogramming. The maintenance of XCI upon reprogramming allows the generation of isogenic iPSC lines that are advantageous for modelling X-linked disorders for several reasons. In fact, clones expressing the mutated allele are genetically identical to those expressing the wild type one that can be thus used as “healthy controls”. In this way it is possible to eliminate the potentially confounding effect due to the diversity of genetic background existing between individuals and to analyse the “pure” effect of the mutation. Moreover, isogenic iPSCs represent a good system that overcomes the functional mosaicism resulting from XCI in classic human patients culture systems such as fibroblasts, leukocytes, etc (Results 1).

Starting from the fact that mutations in *MECP2* and *CDKL5* genes result in a similar phenotype and that the two proteins are thought to belong to the same molecular pathway we decided to verify whether *CDKL5*-derived neurons showed morphological alterations similar to those reported for *MECP2* neurons. In particular, we focused our attention on previous results on soma size analysis of *MECP2*-mutated neurons, reporting a reduction in soma size in both mouse models and iPSCs-derived neurons as compared to normal controls. However, since the accurate delineation of soma boundaries is difficult, we decided to evaluate nuclear size as an alternative measure. Preliminary analysis on iPSCs-derived neurons from one of our patients did not show any significant difference in *CDKL5*-mutated neurons compared to normal controls. This observation however is not the consequence of the method used (nuclear size measurement instead than soma size); in fact, nuclear size analysis performed in parallel on *MECP2*-iPSCs derived neurons, used as an internal positive control, gave results consistent with previous findings in both *Mecp2*^{-/-} mice and postmortem brain tissues from RTT patients^{59,84} and with the data obtained by other groups for *MECP2*-iPSCs derived neurons^{63,76}. Taken together these preliminary data confirm the accuracy of the method and of the protocol used for neuronal differentiation. Starting from these outcomes it will be

essential to further extend the analysis to other iPSCs clones from both reprogrammed patients in order to confirm the results.

Neuronal differentiation of iPSCs results in variable and heterogeneous cultures, with only a 30-40% of neuronal cells and the remaining population being composed of undifferentiated cells of unknown identity. This heterogeneity, and the difficulty to distinguish isolated neurons in the dense cell network arising in culture, greatly complicate analyses aimed at evaluating neuronal morphology. To overcome these problems we decided to set up a protocol based on the infection of neuronal cells with lentiviral vectors driving GFP expression in order to selectively isolate and visualize single neurons for morphological analysis. To this aim we tested different amounts of lentiviral viruses and different timing of infection and we could finally set up good conditions for neuronal morphology visualization and dendritic spines analysis. Interestingly, from the observation of our neuronal cultures we could notice the presence of some neurons lacking visible spines. This could be due to the fact that these cells express a low amount of GFP not sufficient to visualize spines. However, comparison with neurons presenting spines on the same slides did not evidence important differences in the intensity of GFP staining. It seems thus more likely that these cells are immature neurons, in accordance with recent literature data that indicate that only a fraction of neurons present in culture at the end of in vitro differentiation protocols are really mature^{68,93}. Although *CDKL5* is involved in neurological disorders, its function inside the neuron and the underlying molecular mechanisms of disease remain still uncharacterized, mainly due to the unavailability of both a mouse model and a good human cellular model. *CDKL5* is a kinase protein but few target molecules have been identified so far. Phosphorylation is an essential mechanism for the fine tuning of activity of proteins involved in virtually all cellular processes. Among the others, kinase proteins are essential regulators of signalling cascades regulating gene expression⁹⁴. Considering that the other 2 genes associated to Rett syndrome (*MECP2* and *FOXG1*) are transcriptional regulators, we hypothesized that *CDKL5* signalling might also be important for gene expression regulation. The recent finding of a possible *CDKL5* role in nuclear speckles organization further suggested a potential role for *CDKL5* in mechanisms regulating gene expression¹⁴. Starting from these considerations, we decided to perform gene expression profiling on iPSC clones derived from two *CDKL5* mutated patients, in order to identify candidate genes that might be involved in neurogenetic processes and thus play a possible role in the pathophysiology of *CDKL5*-related disorders. We decided to start from patients iPSCs rather than fibroblasts or leukocytes since for the female patient we have obtained isogenic clones expressing exclusively the WT or mutated *CDKL5* allele; these

clones are genetically identical, except for *CDKL5* expression and they thus allow to overcome the effect of the unpredictable pattern of XCI in other cell types.

Analysis of our data led to the identification of a particularly interesting gene, *GRIP1*. This gene, whose transcript was down-regulated in our study, encodes for a 7-PDZ domain-containing protein that is present in glutamatergic and GABAergic synapses and interacts with the GluR2/3/4c subunits of the AMPA receptors. This interaction seems to play an important role in the postsynaptic accumulation of AMPA receptors and in the plasticity of glutamatergic synapses^{95,96}. Moreover GRIP1 is also able to interact with a wide range of molecules including the Ras GEFs, through both its PDZ and other domains. This looks interesting, considering that the Rho and Ras families of small GTPases play a fundamental role in all stages of axonogenesis and coordinate multiple signal transduction pathways with precise spatial control, contributing to the establishment of neuronal cell morphology⁹⁷. This finding is consistent with the recent discovery that *CDKL5* acts as a critical regulator of neuronal morphogenesis through a signalling pathway involving the Rac1 GTPase in rat brain, favouring the hypothesis of a functional relevance of the observed *GRIP1* alteration¹⁵. However it will be necessary to confirm GRIP1 down-regulation by different approaches (Real Time and western blot experiments) and in a larger number of iPSC clones. Moreover, it will be essential to perform the analysis in neuronal cultures. In fact, we are aware that iPSCs are not the optimal cell type to analyse, since *CDKL5* is involved in primarily neurological disorders. However the current neuronal differentiation protocols yield heterogeneous cell populations that are likely to hamper reliable quantitative analyses. In order to perform reliable expression profiling experiments on iPSCs-derived human *CDKL5*-mutated neurons it will thus be important to isolate relatively pure neuronal populations. Attempts to address this issue are already ongoing. For example, Yuan SH and colleagues recently identified a set of cell surface signatures enabling the isolation of pure viable populations of neuronal stem cells, neurons and glia⁹⁸. Starting from these data we plan to apply this procedure on neuronal cultures and test whether we can obtain viable cultures of isolated neurons for expression profiling.

In conclusion we have established a promising human model for the study of *CDKL5*-related disorders. Our data demonstrate that *CDKL5*-iPS cells can be differentiated into neurons, apparently with the same order and timing of neurogenesis of hESCs and normal brain development thus suggesting that *CDKL5* absence does not influence the initial phases of neuronal fate specification (Results 1 and 2). Preliminary analyses on iPSCs-derived

neurons have not revealed any significant difference in *CDKL5*-mutated neurons compared to normal controls as concerns the nuclear size. Further analyses on additional clones from both patients and eventually additional patients will be essential to confirm the results. Moreover, the detailed characterization of the neuronal differentiation course will allow to identify possible alterations in *CDKL5*-derived neurons and to assess whether the alterations recently reported in rat neurons can be confirmed in human cells¹⁵. To this aim we have set up a protocol for the analysis of neuronal morphology based on the use of a lentivirus expressing GFP specifically in neurons (Results2). Finally, preliminary expression profiling experiments in iPSCs revealed an interesting gene that will deserve additional validation on iPSCs-derived neurons (Results3).

5. REFERENCES

5. References

- 1 Montini E, Andolfi G, Caruso A *et al*: Identification and characterization of a novel serine-threonine kinase gene from the Xp22 region. *Genomics* 1998; **51**: 427-433.
- 2 Kalscheuer VM, Tao J, Donnelly A *et al*: Disruption of the serine/threonine kinase 9 gene causes severe X-linked infantile spasms and mental retardation. *Am J Hum Genet* 2003; **72**: 1401-1411.
- 3 Lin C, Franco B, Rosner MR: CDKL5/Stk9 kinase inactivation is associated with neuronal developmental disorders. *Hum Mol Genet* 2005; **14**: 3775-3786.
- 4 Fichou Y, Nectoux J, Bahi-Buisson N, Chelly J, Bienvenu T: An isoform of the severe encephalopathy-related CDKL5 gene, including a novel exon with extremely high sequence conservation, is specifically expressed in brain. *J Hum Genet* 2011; **56**: 52-57.
- 5 Williamson SL, Giudici L, Kilstrup-Nielsen C *et al*: A novel transcript of cyclin-dependent kinase-like 5 (CDKL5) has an alternative C-terminus and is the predominant transcript in brain. *Hum Genet* 2011.
- 6 Mari F, Azimonti S, Bertani I *et al*: CDKL5 belongs to the same molecular pathway of MeCP2 and it is responsible for the early-onset seizure variant of Rett syndrome. *Hum Mol Genet*. 2005; **14**: 1935-1946.
- 7 Bertani I, Rusconi L, Bolognese F *et al*: Functional consequences of mutations in CDKL5, an X-linked gene involved in infantile spasms and mental retardation. *J Biol Chem* 2006; **281**: 32048-32056.
- 8 Carouge D, Host L, Aunis D, Zwiller J, Anglard P: CDKL5 is a brain MeCP2 target gene regulated by DNA methylation. *Neurobiol Dis* 2010; **38**: 414-424.
- 9 Kameshita I, Sekiguchi M, Hamasaki D *et al*: Cyclin-dependent kinase-like 5 binds and phosphorylates DNA methyltransferase 1. *Biochem Biophys Res Commun* 2008; **377**: 1162-1167.
- 10 Shahbazian M, Zoghbi H: Rett Syndrome and MeCP2: Linking Epigenetics and Neuronal Function. *Am J Hum Genet* 2002; **71**: 1259-1272.
- 11 Jung BP, Jugloff DG, Zhang G, Logan R, Brown S, Eubanks JH: The expression of methyl CpG binding factor MeCP2 correlates with cellular differentiation in the developing rat brain and in cultured cells. *J Neurobiol* 2003; **55**: 86-96.
- 12 Mullaney B, Johnston M, Blue M: Developmental expression of methyl-CpG binding protein 2 is dynamically regulated in the rodent brain. *Neuroscience* 2004; **123**: 939-949.
- 13 Rusconi L, Salvatoni L, Giudici L *et al*: CDKL5 expression is modulated during neuronal development and its subcellular distribution is tightly regulated by the C-terminal tail. *J Biol Chem* 2008; **283**: 30101-30111.
- 14 Ricciardi S, Kilstrup-Nielsen C, Bienvenu T, Jacquette A, Landsberger N, Broccoli V: CDKL5 influences RNA splicing activity by its association to the nuclear speckle molecular machinery. *Hum Mol Genet* 2009; **18**: 4590-4602.
- 15 Chen Q, Zhu YC, Yu J *et al*: CDKL5, a protein associated with rett syndrome, regulates neuronal morphogenesis via Rac1 signaling. *J Neurosci* 2010; **30**: 12777-12786.
- 16 Tao J, Van Esch H, Hagedorn-Greiwe M *et al*: Mutations in the X-linked cyclin-dependent kinase-like 5 (CDKL5/STK9) gene are associated with severe neurodevelopmental retardation. *Am J Hum Genet*. 2004; **75**: 1149-1154.

- 17 Weaving L, Christodoulou J, Williamson S *et al*: Mutations of CDKL5 cause a severe neurodevelopmental disorder with infantile spasms and mental retardation. *Am J Hum Genet*. 2004; **75**: 1079-1093.
- 18 Scala E, Ariani F, Mari F *et al*: CDKL5/STK9 is mutated in Rett syndrome variant with infantile spasms. *J Med Genet* 2005; **42 (2)**: 103-107.
- 19 Van Esch H, Jansen A, Bauters M, Froyen G, Fryns JP: Encephalopathy and bilateral cataract in a boy with an interstitial deletion of Xp22 comprising the CDKL5 and NHS genes. *Am J Med Genet A* 2007; **143**: 364-369.
- 20 Archer HL, Evans J, Edwards S *et al*: CDKL5 mutations cause infantile spasms, early onset seizures, and severe mental retardation in female patients. *J Med Genet* 2006; **43**: 729-734.
- 21 Bahi-Buisson N, Kaminska A, Boddaert N *et al*: The three stages of epilepsy in patients with CDKL5 mutations. *Epilepsia* 2008; **49**: 1027-1037.
- 22 Hagberg BA, Skjeldal OH: Rett variants: a suggested model for inclusion criteria. *Pediatr Neurol* 1994; **11**: 5-11.
- 23 Temudo T, Maciel P, Sequeiros J: Abnormal movements in Rett syndrome are present before the regression period: a case study. *Mov Disord* 2007; **22**: 2284-2287.
- 24 Artuso R: Early-onset seizure variant of Rett syndrome: Definition of the clinical diagnostic criteria. *Brain and Development* 2010; **32**: 17-24.
- 25 Bahi-Buisson N, Nectoux J, Rosas-Vargas H *et al*: Key clinical features to identify girls with CDKL5 mutations. *Brain* 2008; **131**: 2647-2661.
- 26 Buoni S, Zannolli R, Colamaria V *et al*: Myoclonic encephalopathy in the CDKL5 gene mutation. *Clin Neurophysiol* 2006; **117**: 223-227.
- 27 Hagberg B, Hanefeld F, Percy A, Skjeldal O: An update on clinically applicable diagnostic criteria in Rett syndrome. Comments to Rett Syndrome Clinical Criteria Consensus Panel Satellite to European Paediatric Neurology Society Meeting, Baden Baden, Germany, 11 September 2001. *Eur J Paediatr Neurol* 2002; **6**: 293-297.
- 28 Chahrour M, Zoghbi HY: The story of Rett syndrome: from clinic to neurobiology. *Neuron* 2007; **56**: 422-437.
- 29 Hagberg B, Aicardi J, Dias K, Ramos O: A progressive syndrome of autism, dementia, ataxia, and loss of purposeful hand use in girls: Rett's syndrome: report of 35 cases. *Ann Neurol* 1983; **14**: 471-479.
- 30 Weaving LS, Ellaway CJ, Gecz J, Christodoulou J: Rett syndrome: clinical review and genetic update. *J Med Genet* 2005; **42**: 1-7.
- 31 Matijevec T, Knezevic J, Slavica M, Pavelic J: Rett syndrome: from the gene to the disease. *Eur Neurol* 2009; **61**: 3-10.
- 32 Christodoulou J, Grimm A, Maher T, Bennetts B: RettBASE: The IRSA MECP2 variation database-a new mutation database in evolution. *Hum Mutat* 2003; **21**: 466-472.
- 33 Sampieri K, Meloni I, Scala E *et al*: Italian Rett database and biobank. *Hum Mutat* 2007; **28**: 329-335.
- 34 Archer HL, Whatley SD, Evans JC *et al*: Gross rearrangements of the MECP2 gene are found in both classical and atypical Rett syndrome patients. *J Med Genet* 2006; **43**: 451-456.
- 35 Jan MM, Dooley JM, Gordon KE: Male Rett syndrome variant: application of diagnostic criteria. *Pediatr Neurol* 1999; **20**: 238-240.
- 36 Ravn K, Nielsen JB, Uldall P, Hansen FJ, Schwartz M: No correlation between phenotype and genotype in boys with a truncating MECP2 mutation. *J Med Genet* 2003; **40**: e5.
- 37 Kleefstra T, Yntema HG, Nillesen WM *et al*: MECP2 analysis in mentally retarded patients: implications for routine DNA diagnostics. *Eur J Hum Genet* 2004; **12**: 24-28.

- 38 Clayton-Smith J, Watson P, Ramsden S, Black GC: Somatic mutation in MECP2 as a non-fatal neurodevelopmental disorder in males. *Lancet* 2000; **356**: 830-832.
- 39 Schwartzman J, Bernardino A, Nishimura A, Gomes R, Zatz M: Rett syndrome in a boy with a 47,XXY karyotype confirmed by a rare mutation in the MECP2 gene. *Neuropediatrics* 2001; **32**: 162-164.
- 40 Meloni I, Bruttini M, Longo I *et al*: A mutation in the Rett syndrome gene, *MECP2*, causes X-linked mental retardation and progressive spasticity in males. *Am J Hum Genet* 2000; **67**: 982-985.
- 41 Cohen D, Lazar G, Couvert P *et al*: MECP2 mutation in a boy with language disorder and schizophrenia. *Am J Psychiatry* 2002; **159**: 149-149.
- 42 Lundvall M, Samuelsson L, Kyllerman M: Male Rett phenotypes in T158M and R294X MeCP2-mutations. *Neuropediatrics* 2006; **37**: 296-301.
- 43 Van Esch H, Bauters M, Ignatius J *et al*: Duplication of the MECP2 Region Is a Frequent Cause of Severe Mental Retardation and Progressive Neurological Symptoms in Males. *Am J Hum Genet* 2005; **77** (3): 442-453.
- 44 Friez MJ, Jones JR, Clarkson K *et al*: Recurrent infections, hypotonia, and mental retardation caused by duplication of MECP2 and adjacent region in Xq28. *Pediatrics* 2006; **118**: e1687-1695.
- 45 Ariani F, Hayek G, Rondinella D *et al*: FOXP1 is responsible for the congenital variant of Rett syndrome. *Am J Hum Genet* 2008; **83**: 89-93.
- 46 Philippe C, Amsellem D, Francannet C *et al*: Phenotypic variability in Rett syndrome associated with FOXP1 mutations in females. *J Med Genet* 2009.
- 47 Mencarelli MA, Spanhol-Rosseto A, Artuso R *et al*: Novel FOXP1 mutations associated with the congenital variant of Rett syndrome. *J Med Genet* 2010; **47**: 49-53.
- 48 Bahi-Buisson N, Nectoux J, Girard B *et al*: Revisiting the phenotype associated with FOXP1 mutations: two novel cases of congenital Rett variant. *Neurogenetics* 2010; **11**: 241-249.
- 49 Le Guen T, Bahi-Buisson N, Nectoux J *et al*: A FOXP1 mutation in a boy with congenital variant of Rett syndrome. *Neurogenetics* 2010.
- 50 Kriaucionis S, Bird A: The major form of MeCP2 has a novel N-terminus generated by alternative splicing. *Nucleic Acids Res.* 2004; **32**: 1818-1823.
- 51 Mnatzakanian GN, Lohi H, Munteanu I *et al*: A previously unidentified MECP2 open reading frame defines a new protein isoform relevant to Rett syndrome. *Nat Genet* 2004; **36**: 339-341.
- 52 Klose RJ, Sarraf SA, Schmiedeberg L, McDermott SM, Stancheva I, Bird AP: DNA binding selectivity of MeCP2 due to a requirement for A/T sequences adjacent to methyl-CpG. *Mol Cell* 2005; **19**: 667-678.
- 53 Kokura K, Kaul S, Wadhwa R *et al*: The Ski protein family is required for MeCP2-mediated transcriptional repression. *J Biol Chem.* 2001; **276**: 34115-34121.
- 54 Nan X, Ng H, Johnson C *et al*: Transcriptional repression by the methyl-CpG-binding protein MeCP2 involves a histone deacetylase complex. *Nature* 1998; **393**: 386-389.
- 55 Yu F, Thiesen J, Stratling WH: Histone deacetylase-independent transcriptional repression by methyl-CpG-binding protein 2. *Nucleic Acids Res* 2000; **28**: 2201-2206.
- 56 Young JI, Hong EP, Castle JC *et al*: Regulation of RNA splicing by the methylation-dependent transcriptional repressor methyl-CpG binding protein 2. *Proc Natl Acad Sci U S A* 2005; **102**: 17551-17558.
- 57 Yasui DH, Peddada S, Bieda MC *et al*: Integrated epigenomic analyses of neuronal MeCP2 reveal a role for long-range interaction with active genes. *Proc Natl Acad Sci U S A* 2007; **104**: 19416-19421.

- 58 Guy J, Hendrich B, Holmes M, Martin JE, Bird A: A mouse *Mecp2*-null mutation causes neurological symptoms that mimic Rett syndrome. *Nat Genet* 2001; **27**: 322-326.
- 59 Chen RZ, Akbarian S, Tudor M, Jaenisch R: Deficiency of methyl-CpG binding protein-2 in CNS neurons results in a Rett-like phenotype in mice. *Nature Genetics* 2001; **27**: 327-331.
- 60 Chao HT, Zoghbi HY, Rosenmund C: MeCP2 controls excitatory synaptic strength by regulating glutamatergic synapse number. *Neuron* 2007; **56**: 58-65.
- 61 Ballas N, Lioy DT, Grunseich C, Mandel G: Non-cell autonomous influence of MeCP2-deficient glia on neuronal dendritic morphology. *Nat Neurosci* 2009; **12**: 311-317.
- 62 Yao J, Lai E, Stifani S: The winged-helix protein brain factor 1 interacts with groucho and hes proteins to repress transcription. *Mol Cell Biol* 2001; **21**: 1962-1972.
- 63 Marchetto MC, Carromeu C, Acab A *et al*: A model for neural development and treatment of Rett syndrome using human induced pluripotent stem cells. *Cell* 2010; **143**: 527-539.
- 64 Takahashi K, Tanabe K, Ohnuki M *et al*: Induction of pluripotent stem cells from adult human fibroblasts by defined factors. *Cell* 2007; **131**: 861-872.
- 65 Takahashi K, Okita K, Nakagawa M, Yamanaka S: Induction of pluripotent stem cells from fibroblast cultures. *Nat Protoc* 2007; **2**: 3081-3089.
- 66 Maherali N, Sridharan R, Xie W *et al*: Directly reprogrammed fibroblasts show global epigenetic remodeling and widespread tissue contribution. *Cell Stem Cell* 2007; **1**: 55-70.
- 67 Hanna J, Cheng AW, Saha K *et al*: Human embryonic stem cells with biological and epigenetic characteristics similar to those of mouse ESCs. *Proc Natl Acad Sci U S A* 2010; **107**: 9222-9227.
- 68 Hu BY, Weick JP, Yu J *et al*: Neural differentiation of human induced pluripotent stem cells follows developmental principles but with variable potency. *Proc Natl Acad Sci U S A* 2010; **107**: 4335-4340.
- 69 Swistowski A, Peng J, Liu Q *et al*: Efficient generation of functional dopaminergic neurons from human induced pluripotent stem cells under defined conditions. *Stem Cells* 2010; **28**: 1893-1904.
- 70 Yan Y, Yang D, Zarnowska ED *et al*: Directed differentiation of dopaminergic neuronal subtypes from human embryonic stem cells. *Stem Cells* 2005; **23**: 781-790.
- 71 Johnson MA, Weick JP, Pearce RA, Zhang SC: Functional neural development from human embryonic stem cells: accelerated synaptic activity via astrocyte coculture. *J Neurosci* 2007; **27**: 3069-3077.
- 72 Li XJ, Du ZW, Zarnowska ED *et al*: Specification of motoneurons from human embryonic stem cells. *Nat Biotechnol* 2005; **23**: 215-221.
- 73 Pankratz MT, Li XJ, Lavaute TM, Lyons EA, Chen X, Zhang SC: Directed neural differentiation of human embryonic stem cells via an obligated primitive anterior stage. *Stem Cells* 2007; **25**: 1511-1520.
- 74 Swistowski A, Peng J, Han Y, Swistowska AM, Rao MS, Zeng X: Xeno-free defined conditions for culture of human embryonic stem cells, neural stem cells and dopaminergic neurons derived from them. *PLoS One* 2009; **4**: e6233.
- 75 Tchieu J, Kuoy E, Chin MH *et al*: Female human iPSCs retain an inactive X chromosome. *Cell Stem Cell* 2010; **7**: 329-342.
- 76 Cheung AY, Horvath LM, Grafodatskaya D *et al*: Isolation of MECP2-null Rett Syndrome patient hiPS cells and isogenic controls through X-chromosome inactivation. *Hum Mol Genet* 2011; **20**: 2103-2115.

- 77 Ebert AD, Yu J, Rose FF, Jr. *et al*: Induced pluripotent stem cells from a spinal muscular atrophy patient. *Nature* 2008.
- 78 Lee G, Studer L: Modelling familial dysautonomia in human induced pluripotent stem cells. *Philos Trans R Soc Lond B Biol Sci* 2009; **366**: 2286-2296.
- 79 Marchetto MC, Winner B, Gage FH: Pluripotent stem cells in neurodegenerative and neurodevelopmental diseases. *Hum Mol Genet* 2010; **19**: R71-76.
- 80 Vaccarino FM, Stevens HE, Kocabas A *et al*: Induced pluripotent stem cells: a new tool to confront the challenge of neuropsychiatric disorders. *Neuropharmacology* 2011; **60**: 1355-1363.
- 81 Armstrong D, *al e*: Selective dendritic alterations in the cortex of Rett syndrome. *Nuropathol Exp Neurol* 1995; **54**: 195-201.
- 82 Rosas-Vargas H, Bahi-Buisson N, Philippe C *et al*: Impairment of CDKL5 nuclear localisation as a cause for severe infantile encephalopathy. *J Med Genet* 2008; **45**: 172-178.
- 83 Kaufmann WE, Moser HW: Dendritic anomalies in disorders associated with mental retardation. *Cereb Cortex* 2000; **10**: 981-991.
- 84 Bauman ML, Kemper TL: Neuroanatomic observations of the brain in autism: a review and future directions. *Int J Dev Neurosci* 2005; **23**: 183-187.
- 85 Li XJ, Zhang X, Johnson MA, Wang ZB, Lavaute T, Zhang SC: Coordination of sonic hedgehog and Wnt signaling determines ventral and dorsal telencephalic neuron types from human embryonic stem cells. *Development* 2009; **136**: 4055-4063.
- 86 Urdinguio RG, Lopez-Serra L, Lopez-Nieva P *et al*: Mecp2-null mice provide new neuronal targets for Rett syndrome. *PLoS ONE* 2008; **3**: e3669.
- 87 Nectoux J, Fichou Y, Rosas-Vargas H *et al*: Cell cloning-based transcriptome analysis in Rett patients: relevance to the pathogenesis of Rett syndrome of new human MeCP2 target genes. *J Cell Mol Med* 2010; **14**: 1962-1974.
- 88 Delgado IJ, Kim DS, Thatcher KN, LaSalle JM, Van den Veyver IB: Expression profiling of clonal lymphocyte cell cultures from Rett syndrome patients. *BMC Med Genet* 2006; **7**: 61.
- 89 Traynor J, Agarwal P, Lazzeroni L, Francke U: Gene expression patterns vary in clonal cell cultures from Rett syndrome females with eight different MECP2 mutations. *BMC Med Genet* 2002; **3**: 12.
- 90 Colantuoni C, Jeon O-E, Hyder K *et al*: Gene expression profiling in postmortem Rett syndrome brain: differential gene expression and patient classification. *Neurobiol Disease* 2001; **8**: 847-865.
- 91 Tudor M, Akbarian S, Chen RZ, Jaenisch R: Transcriptional profiling of a mouse model for Rett syndrome reveals subtle transcriptional changes in the brain. *Proc Natl Acad Sci U S A* 2002; **99**: 15536-15541.
- 92 Nectoux J, Fichou Y, Cagnard N *et al*: Cell cloning-based transcriptome analysis in cyclin-dependent kinase-like 5 mutation patients with severe epileptic encephalopathy. *J Mol Med (Berl)* 2011; **89**: 193-202.
- 93 Chamberlain SJ, Chen PF, Ng KY *et al*: Induced pluripotent stem cell models of the genomic imprinting disorders Angelman and Prader-Willi syndromes. *Proc Natl Acad Sci U S A* 2010; **107**: 17668-17673.
- 94 Stewart R, Flechner L, Montminy M, Berdeaux R: CREB Is Activated by Muscle Injury and Promotes Muscle Regeneration. *PLoS One* 2011; **6**: e24714.
- 95 Brecht DS, Nicoll RA: AMPA receptor trafficking at excitatory synapses. *Neuron* 2003; **40**: 361-379.
- 96 Li RW, Serwanski DR, Miralles CP *et al*: GRIP1 in GABAergic synapses. *J Comp Neurol* 2005; **488**: 11-27.

- 97 Hall A, Lalli G: Rho and Ras GTPases in axon growth, guidance, and branching. *Cold Spring Harb Perspect Biol* 2010; **2**: a001818.
- 98 Yuan SH, Martin J, Elia J *et al*: Cell-surface marker signatures for the isolation of neural stem cells, glia and neurons derived from human pluripotent stem cells. *PLoS One* 2011; **6**: e17540.

Acknowledgements

During this journey called PhD I've met several people. Everybody has played an important role in this experience and everybody would deserve some words of acknowledgements.

I want to thank Prof. Alessandra Renieri for giving me the opportunity to join her lab 4 years ago and for believing in me. Working on such interesting research projects during these years has contributed to increase my technical skills and scientific thinking and has confirmed my strong motivation to continue my working career in science.

A special thanks to the "Medical Genetics Girls", with whom I shared not only science but also several nice moments outside the "blu door".

I want to thank Francesca Ariani for helping me taking my first steps in the laboratory and following me in the first two years of my PhD with her suggestions and advices.

A thank to Ilaria Meloni for all the professional teachings I've received working with her and for the insightful scientific discussions that have contributed to improve my scientific thinking and grow up as a scientist, I hope!

I would like to thank my friend and colleague Roberta for the reciprocal encouragements during these 4 years, for the bad and good moments inside the "cell culture room" and for each moment outside during our innumerable life experiences.

A special thank to all my friends old and new ("the Campansi group") that have supported me during these years and joined with me several happy and sad moments! Thank you for encouraging me to never give up and to not to be afraid of trying to pursue my dreams. I'm not going to write any name.....the list is too long and all of you know exactly how much I love you.

Finally my grateful thought goes to my parents and to my sisters Antonella and Gabriella, far away from me but always close to my heart. Thank you for sustaining me in every choice and trusting me in every single moment.